JAHRBUCH DER GEOLOGISCHEN BUNDESANSTALT

Jb. Geol. B.-A. | ISSN 0016–7800 | Band 143 | Heft 1 | S. 23–38 | Wien, März 2003

Chemical and Structural Evolution of Chlorites and White K-Micas in Various Lithologies of the Low-Grade Graz Paleozoic (Eastern Alps, Austria)

PÉTER ÁRKAI*), ALOIS FENNINGER**) & GÉZA NAGY*)

8 Text-Figures and 7 Tables

Grazer Paläozoikum
Niedriggradige Metamorphose
Metabasite
Metatuffite
Metapelite

Österreichische Karte 1 : 50.000
Blätter 134, 135, 164, 165, 190

Inhalt

Chemische und strukturelle Evolution von Chloriten und Hellglimmern in verschiedenen Gesteinen des niedrig metamorphen Grazer Paläozoikums (Ostalpen, Österreich)

Zusammenfassung

Aus dem Grazer Paläozoikum werden neue Daten zur chemischen und strukturellen Entwicklung von Chloriten und Hellglimmern unterschiedlicher Lithologien (pelitisch-mergelige Sedimente, Metatuffite, Laven und untergeordnet basische Intrusivgesteine) aus den einzelnen Deckeneinheiten vorgestellt. Grundsätzlich kann die Chlorit-Kristallinität zur Abschätzung des Diagenese- und Metamorphosegrades in Peliten und Tuffiten herangezogen werden. Gegenüber der Illit-Kristallinität ist sie weniger lithologieabhängig. Die IK in Metatuffiten zeigt gegenüber Metapeliten abnormal hohe Werte. Metabasische Laven und Intrusivgesteine haben sowohl abnormale IK- als auch ChK-Indices.

Neben dem wohlbekannten temperaturgesteuerten Effekt der Abnahme smektitischer Mixed-layer-Mineralien in Illiten-Hellglimmern beeinflusst auch der Seladonit-Gehalt in starkem Maße die IK. Sie ist wesentlich vom Gesamtgesteinschemismus abhängig und korreliert vor allem mit dem $Al_2O_3/(Al_2O_3+FeO^*+MgO)$-Verhältnis. Die ChK spiegelt die Anteile an quellfähigen Mixed-layer-Mineralien und dioctahedraler (sudoitischer) Substitutionen wider, während die Fe/Mg-Verhältnisse keinen nennenswerten Einfluss auf die ChK haben.

Daraus folgt, dass der Gesamtgesteinschemismus (Hauptelemente) und die mineralchemischen Relationen mitberücksichtigt werden müssen, um Kristallinitäts-Indices von Phyllosilicaten verschiedenster Lithologien zur Erfassung der Diagenese und beginnenden Metamorphose heranzuziehen.

Abstract

Reaction progresses of chlorite and white K-mica from various lithologies (pelitic-marly metasedimentary rocks, metatuffites, lava and subordinately, intrusive rocks of mostly basic composition) are compared using XRD, EMP and bulk rock major element composition data. The sample series derives from various nappes of the Graz Paleozoic, Upper Austroalpine Nappe System. The grades of mostly Variscan regional alteration of the Silurian and Devonian samples span between late diagenesis (prehnite-pumpellyite facies) and epizone (greenschist facies), representing mainly the anchizone.

Obvious discrepancies found between the EMP data (obtained necessarily from larger grains or aggregates) and XRD properties of <2 μm fraction samples prove metastable inequilibrium conditions. XRD illite crystallinity (IC) indices measured on air-dried and glycolated mounts refer to decreasing amounts of swelling mixed-layers with increasing grade. By contrast, no correlation was found between IC and total interlayer charge, indicating that EMP-measured larger authigenic mica flakes reflect a more evolved stage in reaction progress as compared to the matrix-forming finer-grained main population. In addition, IC shows significant positive correlations with celadonite content and with $Fe^{2+}/(Fe^{2+}+Mg)$ ratio, referring to effects of the bulk rock chemistry (lithology).

*) Prof. Dr. PÉTER ÁRKAI, Dr. GÉZA NAGY: Laboratory for Geochemical Research, Hungarian Academy of Sciences, H 1112 Budapest, Budaörsi út 45, Hungary.
**) Univ.-Prof. Dr. ALOIS FENNINGER: Karl-Franzens-University Graz, Institute of Geology and Paleontology, A 8010 Graz, Heinrichstraße 26, Austria.

Differences in ChC indices measured on air-dried, glycolated and Mg-saturated mounts refer to subordinate amounts of swelling mixed-layers in chlorite, the amounts of which seem to decrease with advancing grade. EMP data from larger grains or aggregates represent a more evolved stage than that indirectly implied for matrix-forming chlorite from XRD data. Chlorite end member ratios were calculated from those analyses which prove a poor chloritic phase (Ca+Na+K<0.1 p.f.u.). In addition to the $Fe^{2+}Mg_{-1}$ and Tschermak's substitutions, the di-trioctahedral (sudoitic) substitution plays also an important role in chlorite chemistries. However, the proportion of sudoite end member is generally lower than 20 %. Although the compositional ranges are strongly overlapping, chlorites from metasedimentary rocks are characterized by mostly higher "amesite" and sudoite, chlorites from metabasic lava and intrusive rocks with higher clinochlore + daphnite contents. Chlorites of metatuffites are of intermediate compositions. ChC indices show significant negative correlations with Al^{IV}, and Al^{VI} contents, while no relation was found with Fe^{2+}/Mg ratios.

Thus, in addition to swelling mixed-layered impurities, crystallite size and lattice strain relations, IC and ChC are also influenced by chemistries of illite-muscovite and chlorite, which, in turn, are related to bulk rock compositions. In spite of this, XRD chlorite crystallinity indices proved to be a reliable tool for estimating relative differences in metamorphic grade, when bulk rock chemistries are also taken into consideration.

1. Introduction

Exact determination of grades, facies or zones of low-temperature meta-igneous rocks, including meta-volcanoclastics is hindered by the general lack of index minerals in rocks that transformed in CO_2-containing fluid systems. Diagnostic index minerals such as various zeolites, prehnite and pumpellyite form in fluid systems consisting of H_2O and practically devoid of CO_2 (for reviews see LIOU et al., 1987; FREY et al., 1991; ROBINSON & BEVINS, 1999; ALT, 1999). By contrast, meta-igneous rocks of basic to intermediate chemistries and their clastic derivatives that formed in the presence of CO_2-containing fluids commonly comprise mineral assemblages such as quartz, albite, chlorite ± carbonate minerals and various accessories. Such non-diagnostic mineral assemblages are stable over a large temperature range between c. 100–150 and 400–450°C. These rock types are frequently found in ancient continental shelf environment, thus are widespread in many Paleozoic and Mesozoic sequences of the Tethyan realm.

X-ray powder diffractometric (XRD) chlorite crystallinity method was found to be a reliable measure of metamorphic grades, not only for metapelites (ÁRKAI, 1991; YANG & HESSE, 1991; ÁRKAI et al., 1995) but also for meta-igneous rocks of basic to intermediate compositions (ÁRKAI & SADEK GHABRIAL, 1997). ÁRKAI et al. (2000) found that – despite significant differences in composition, mineral assemblages and textures – reaction progress, as measured in part by chlorite crystallinity (ChC), in metapelites paralleled that in metabasites. Mean crystallite size increases, the proportion of (swelling) mixed-layers decreases in chlorites with advancing grade.

In order to test the applicability of the ChC method, meta-igneous rocks and their metasedimentary environments from the Graz Paleozoic and Sausal Paleozoic, Eastern Alps, Austria were studied. The geological history of the Graz Paleozoic is rather well known and documented. The aim of the present paper is to provide new bulk rock chemical, mineral chemical and phyllosilicate crystallinity data on selected rock samples in order to test the applicability of the ChC method for determining the metamorphic grade. Doing this, special attention is paid to the relations between ChC, chlorite chemistry, bulk chemistry and modal composition, i.e., on factors that may significantly influence ChC and thus, may considerably restrict the metamorphic petrogenetic application of chlorite.

2. Geology – Previous Data on Volcanism and Metamorphism

Rock samples studied in the present paper originated from the Graz Paleozoic and Sausal Paleozoic, Eastern Alps, Styria, Austria (Text-Fig. 1). The Graz Paleozoic belongs to the Upper Austroalpine unit and displays a complicated nappe structure. The Rannach and Hochlantsch nappes form the upper, the Laufnitzdorf and Kalkschiefer (Calcschist) nappes the middle and the Schöckel nappe forms the lower units.

These nappes are characterized by various lithologies (Text-Fig. 2). However, all of them contain basic meta-igneous (mostly volcanic lava and pyroclastic) rocks. The Paleozoic volcanism around Graz has been known for more then 180 years ("Trappformation" of VON BUCH, 1819, see in HUBMANN, 1999). The first petrographic descriptions are found in the works of TERGLAV (1876) and HANSEL (1885), see in FLÜGEL (1975), while the first chemical analyses were done by WELISCH (1911). Volcanic rocks are commonly found in association with Silurian and Devonian sedimentary rocks (generally, up to the Middle or Upper Devonian), indicating the time-span of magmatism.

Recent magma-genetic works carried out on the volcanic rocks of the Graz Paleozoic concern mostly the upper nappe unit (KOLMER, 1978; FRITZ & NEUBAUER, 1988, 1990; LOESCHKE, 1989; WEBER, 1990). According to their interpretations, these rocks represent products of intraplate volcanism, the extensional settings of which acted from the Silurian (Kehr Fm.) up to the Middle/Upper Devonian. Within this time-span a shift of volcanism from south towards north has also been observed. The Emsian (upper part of the lower Devonian) volcanoclastic rocks of the Dolomite Sandstone Series characterized by high K_2O contents as compared to Na_2O were sedimented in small, shallow, evaporitic basins of a tidal plane (FLÜGEL & NEUBAUER, 1984). Givetian (upper Middle Devonian) volcanics (mostly meta-alkali basalts and rhyolite tuffs) eventually ranging up to the Upper Devonian are found mainly in the Hochlantsch unit. These are interpreted also as products of intraplate volcanism. Volcanics and their pyroclastics are frequently found also in the lowermost tectonic units of the Graz Paleozoic, i.e., in the Passail and Hochslag Groups (FLÜGEL & NEUBAUER, 1984).

The first results on metamorphism of the Graz Paleozoic are based exclusively on mineral paragenetic observations, related to detailed geological mapping, tectonic and lithofacies studies (THALHAMMER, 1983; NEUBAUER, 1981, 1982; GOLLNER, 1985; HUBAUER, 1984; TSCHELAUT, 1984; FRITZ, 1986; AGNOLI, 1987; REISINGER, 1988; GSELLMANN, 1987; HUBMANN, 1990). The conditions of metamorphism and thermal history of the Graz Paleozoic were reconstructed in detail by RUSSEGGER (1992), HASENHÜTTL & RUSSEGGER (1992) and HASENHÜTTL (1994), on the basis of complex interpretation of vitrinite reflectance, illite crystallinity (IC) measurements carried out on fine-clastic metasedimentary rocks as well as Conodont colour alteration (CAI), microstructural and mineral paragenetic observations (Text-Fig. 3). ChC measurements were carried out on fine-clastic rock only, in a rather restricted way. However, IC and ChC indices showed strong, positive correlation (HASENHÜTTL & RUSSEGGER, 1992).

These studies show an increase of metamorphic grade from East towards North. In the deepest nappe unit epizonal metamorphism was proved. In the middle nappe

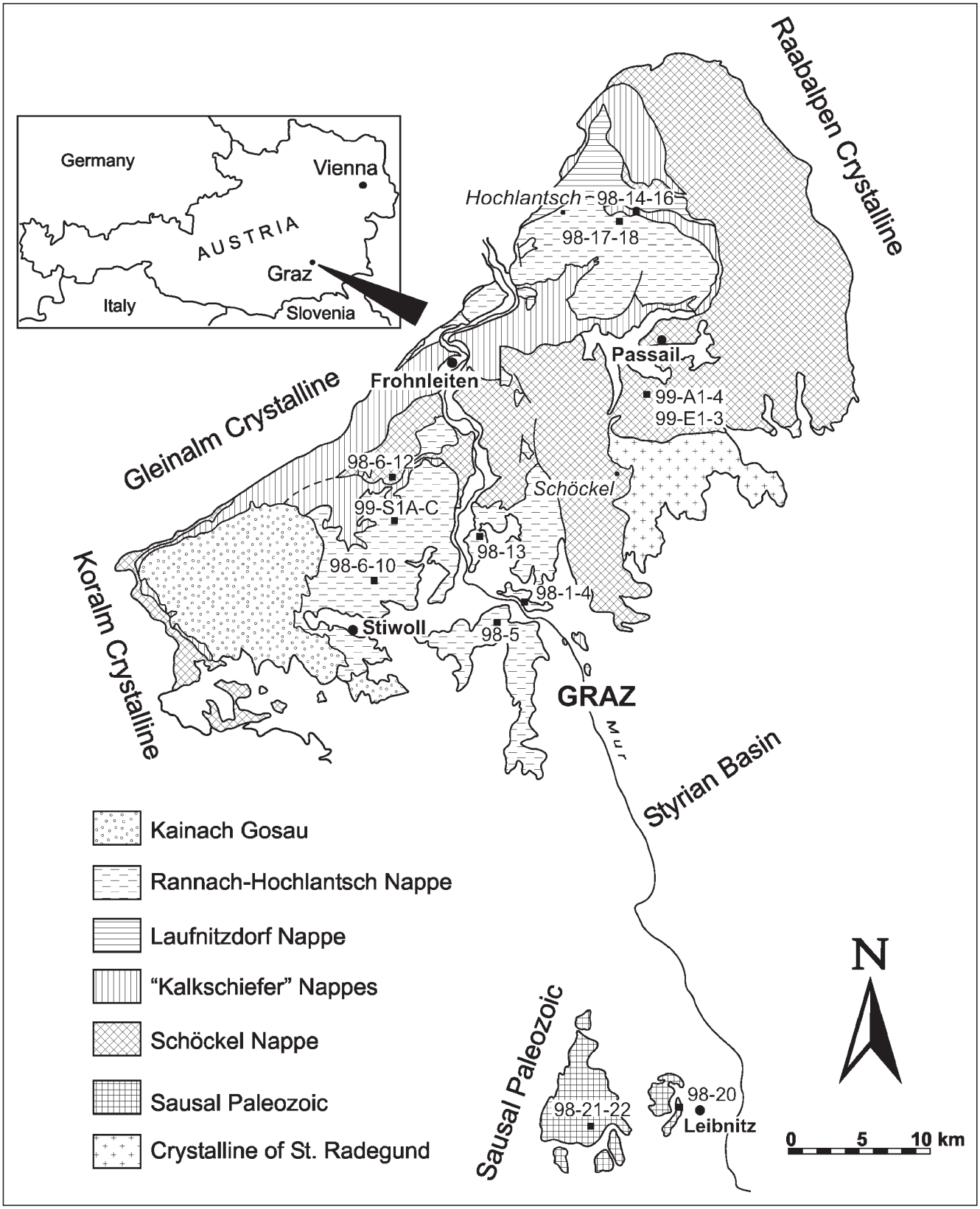

Text-Fig. 1.
Geological sketch map of the Graz Paleozoic, Eastern Alps, Austria.

units the grade of metamorphism seems to be rather heterogeneous: while the mostly anchizonal metamorphic grade of the Laufnitzdorf Unit is comparable to that of the upper nappe unit, the metamorphism in the other units of the Kalkschiefer nappes corresponds to the epizone. Anchizonal metamorphic and diagenetic conditions prevail in the upper nappe units. Here – according to the vitrinite reflectance data – temperature maxima are related to the areas where Silurian–Devonian volcanites are found.

HASENHÜTTL (1994) and HUBMANN & HASENHÜTTL (1995) estimated the following temperature values for the various units: Rannach nappe: up to 250°C in the South and

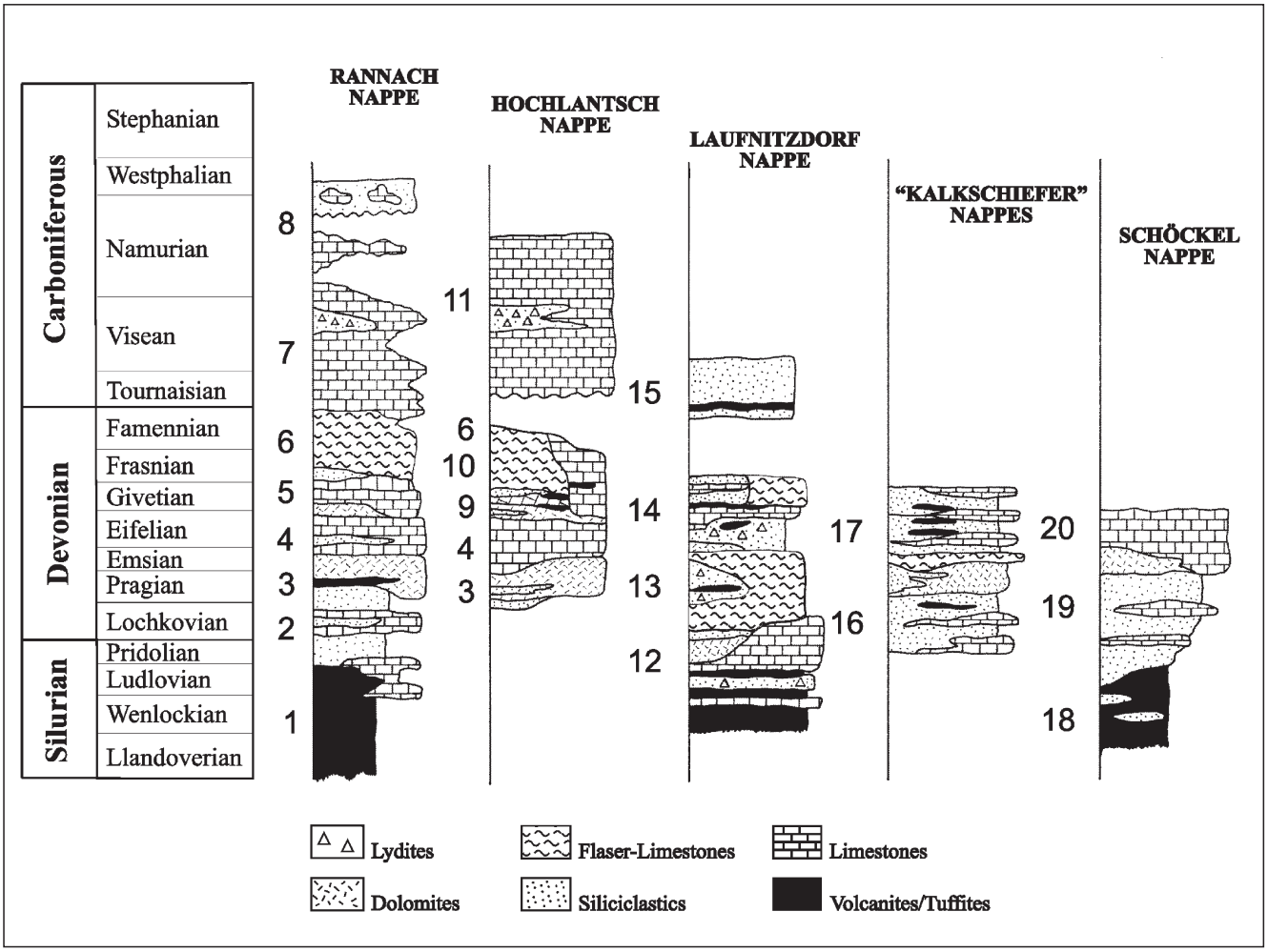

Text-Fig. 2.
Lithological and stratigraphic features of the nappes that built up the Graz Paleozoic.

>300°C in the North; Hochlantsch nappe: max. 350°C (up to the Upper Devonian) and max. 300°C (in the Carboniferous); Laufnitzdorf nappe: max. 320°C; Kalkschiefer and Schöckel nappes: min. 390°C.

3. Materials and Methods

For the present study, metasedimentary (pelitic-marly) rocks associated with metatuffites of basic to intermediate compositions and massive metamagmatic rocks (metabasalts and metagabbro) were collected and selected. Rock types, localities, stratigraphic and tectonic relations of these samples representing mainly the upper and lower tectonic units are summarized in Tab. 1. In addition to the Graz Paleozoic, several samples were collected also from the Sausal Paleozoic located South of Graz, the geological relations of which to the Graz Paleozoic is rather ambiguous.

In order to determine the rock types, their microstructural (textural) features and modal compositions, detailed petrographic microscopic observations were made. In general, the analytical methods applied were similar to those described by ÁRKAI et al. (2000). X-ray powder diffraction

R_{max}(%)	IC (Δ°2Θ)	CAI
1.5 (1.2 - 1.6)	**0.52**	**1 - 2**
6.7 *(6.1 - 7.3)*	***0.24*** *(0.29 - 0.19)*	***5*** *(3 - 7)*
5.3 *(1.9 - 8.8)*	***0.27*** *(0.64 - 0.19)*	**5** (4,5 - 7.5)
5.4 (1.9 - 8.8)	**0.27** (0.64 - 0.19)	**5** (3 - 7.5)
6.4 (4.9 - 7.7)	**0.28** (0.39 - 0.22)	**5** (4 - 6.5)
9.9 (9.3 - 10.4)	**0.21** (0.26 - 0.15)	**5.5** (5 - 7)
9.9 (8.6 - 10.6)	**0.19** (0.22 - 0.16)	**5.5** (5 - 6.5)

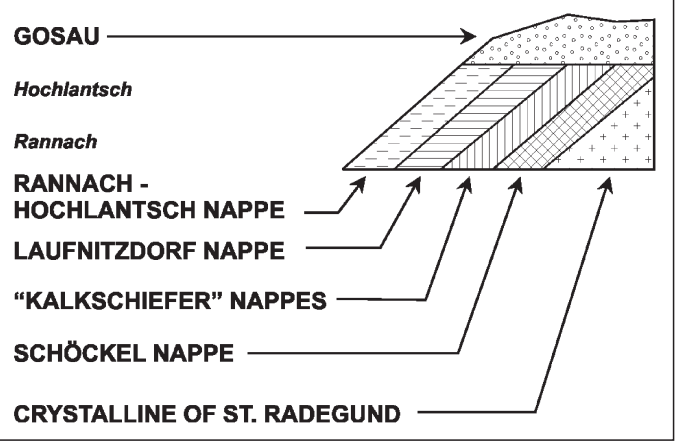

Text-Fig. 3.
Metamorphism of the nappes of the Graz Paleozoic after RUSSEGGER (1992), HASENHÜTTL & RUSSEGGER (1992), HASENHÜTTL (1994) and HUBMANN & HASENHÜTTL (1995).
IC = illite crystallinity index; R_{max}% = maximal vitrinite reflectance; CAI = Conodont colour alteration index.

Table 1.
List and characterization of rock types investigated from the Graz and Sausal Paleozoic.

No. of samples	Rock type	Locality	Lithostratigraphy	Age	Tectonic unit
GP-98-1	marly slate	Admonter Kogel, ÖK:164 Coord: 15°13'19"E/47°06'50"N	Flösserkogel Fm.	Lower Devonian Emsian	Rannach Nappe
GP-98-2 GP-98-3 GP-98-4	metatuffite metatuffite metatuffite	Admonter Kogel, ÖK: 164 Coord: 15°13'19"E/47°06'50"N	Flösserkogel Fm.	Lower Devonian Emsian	Rannach Nappe
GP-98-5	metatuffite	ruin Gösting, ÖK: 164 Coord: 15°22'00"E/47°06'12"N	Flösserkogel Fm.	Lower Devonian Emsian	Rannach Nappe
GP-98-6	slate	Fallentsch, ÖK: 163 Coord: 15°13'00"E/47°07'28"N	Kehr-Vulkanit Fm.	Silurian	Rannach Nappe
GP-98-7	marly slate	Fallentsch, ÖK: 163 Coord: 15°13'00"E/47°07'28"N	Kehr-Vulkanit Fm.	Silurian	Rannach Nappe
GP-98-8	marly slate	Fallentsch, ÖK: 163 Coord: 15°13'00"E/47°07'28"N	Kehr-Vulkanit Fm.	Silurian	Rannach Nappe
GP-98-9 GP-98-10 GP-98-11	metatuffite	Fallentsch, ÖK: 163 Coord: 15°13'00"E/47°07'28"N	Kehr-Vulkanit Fm.	Silurian	Rannach Nappe
GP-98-13	metabasalt	Haritzgraben, ÖK: 164 Coord: 15°26'23"E/47°10'23"N	Kehr-Vulkanit Fm.	Silurian	Rannach Nappe
GP-98-16a GP-98-16b	metabasalt	NW Breitalmkreuz, ÖK: 134 Coord: 15°28'00"E/47°21'28"N	Tyrnaueralm Fm.	Middle Devonian	Hochlantsch Nappe
GP-98-17	metagabbro	NW Breitalmkreuz (Jagdhütte), ÖK: 134 Coord: 15°27'54"E/47°21'28"N	Tyrnaueralm Fm.	Middle Devonian	Hochlantsch Nappe
GP-98-18	metabasalt	NW Breitalmkreuz (Jagdhütte), ÖK: 134 Coord: 15°27'54"E/47°21'28"N	Tyrnaueralm Fm.	Middle Devonian	Hochlantsch Nappe
GP-98-14	silty, marly slate	Russenstrasse, ÖK: 134 Coord: 15°29'00"E/47°22'21"N	? Kogler Fm.	Devonian	Kalkschiefer Nappe
GP-98-15	palitic, marly slate	Russenstrasse, ÖK: 134 Coord: 15°28'13"E/47°21'43"N	? Kogler Fm.	Devonian	Kalkschiefer Nappe
GP-98-12	metabasalt	Waldstein, ÖK: 163 Coord: 15°17'30"E/47°13'23"N	Taschen-Schiefer Fm.	?	Schöckel Nappe
GP-99-S1A GP-99-S1B GP-99-S1C	metatuffite slate metatuffite	Silberberg, ÖK: 163 Coord: 15°13'06"E/47°12'13"N	Taschen-Schiefer Fm.	?	Schöckel Nappe
GP-99-A1 GP-99-A2 GP-99-A3 GP-99-A4	banded, carbonatic metatuffite	Arzberg, ÖK: 134 Coord: 15°31'07"E/47°15'00"N	Schönberg Fm.	Lower Paleozoic	Schöckel Nappe
GP-99-E1 GP-99-E2 GP-99-E3	metatuffite metatuffite metatuffite	Arzberg, ÖK: 134 Coord: 15°31'07"E/47°15'00"N	Schönberg Fm.	Lower Paleozoic	Schöckel Nappe
GP-98-19	quartz phyllite (metasandstone)	Passail, ÖK: 165 Coord: 15°30'11"E/47°16'46"N	Semriach Phyllit Fm.	?	Schöckel Nappe
GP-98-20	phyllite	Seggauberg, ÖK: 190 Coord: 15°31'35"E/46°47'00"N	?	Lower Paleozoic	Sausal Paleozoic
GP-98-21 GP-98-22	greenschist (metatuffite)	Heimschuh, ÖK: 190 Coord: 15°28'54"E/46°46'38"N	?	Lower Paleozoic	Sausal Paleozoic

(XRD) patterns were obtained from both non-oriented and highly oriented powder mounts of whole rock and <2 μm spherical equivalent diameter size fractions. Decarbonation of samples – if it was necessary – preceded the preparation of mounts using cold, 10 % acetic acid that – according to earlier experiments of the authors – did not attack even the Fe-rich variants of chlorite. XRD data were in part used for the determination of modal composition and values of illite crystallinity [IC, i.e. the full width at half-maximum (FWHM) of the first, 10 Å basal reflection of illite-white K-mica] and chlorite crystallinity [ChC, i.e. the FWHM values of the first (14 Å) and second (7 Å) basal reflections of chlorite, denoted as ChC(001) and ChC(002), respectively]. The <2μm fraction samples were prepared by methods similar to that of KÜBLER (1968), as described by ÁRKAI (1991). Portions of the air-dried <2 μm fraction samples were saturated with 0.5 mol^{-1} $MgCl_2$ solutions. Aqueous suspensions were pipetted onto glass slides and dried at room temperature to produce highly oriented mounts having concentrations of 3 mg cm^{-2}. Air-dried (AD), and Mg-saturated and air-dried (Mg,AD) mounts were thus obtained. Ethylene glycol (EG) solvations (80°C/overnight) completed the sample preparation procedure. The XRD instrumental and measuring conditions were: Philips PW-1730 diffractometer with computerized APD system, Cu Kα radiation, 45 kV/35 mA, proportional counter, graphite monochromator, divergence and detector slits of 1°, and collection of data with 0.02°2Θ steps, using time intervals of 5 s. The calibration of IC and ChC values against KÜBLERS IC scale, where values for the anchizone range between 0.25 and 0.42°Δ2Θ, was made using standard rock slab series (Nos. 32, 34 & 35) kindly provided by B. KÜBLER. Smaller scale variations in instrumental conditions were corrected by the repeated use of another calibrated standard rock slab series (Nos. Á-1, -2 & -3) of the Laboratory for Geochemical Research, Budapest.

Table 2.
Modal composition of whole rock samples (results of petrographic microscopic, XRD and EMP investigations)

sample	Qtz	Ab	Kfs	Ill-Ms[1]	Bt	Chl	Chl/Sm	Ill/Sm	Sm	Kln	Cpx	Act	Ep	Pmp	Prh	Cal	Dol	Sid	Py	Hem	Rt	Ilm	Tit	Ap	Goe	Tur
GP-98-1	*x*			*x*													*x*				*x*				*x*	
GP-98-2	x	x	x	x				tr												x						
GP-98-3	x		x	x				tr									tr?			x						
GP-98-4	x	tr?	x	x				tr								tr?	x									
GP-98-5	x	x	x	x				tr	tr											x						
GP-98-6	*x*	*x*		*x*		*x*		*tr*	*tr*							*x*					*x*					
GP-98-7	*x*			*x*		*x*										*x*									*tr*	
GP-98-8	*x*	*x*		*x*			*tr*									*x*					*x*				*tr?*	
GP-98-9	x	x		x		x										x	x*	tr?		x						
GP-98-10	x			x		x										x	x*	x		x	x			x		
GP-98-11	x	x		tr		x										x				x	x					
GP-98-13	**x**	**x**		**x**		**x**					**x**	**x**	**x**		**tr?**	**tr?**	**x**	**tr?**		**tr?**	**tr?**		**tr?**			
GP-98-16a	**x**	**x**	**x**	**x**		**x**					**x**	**x**	**x**		**x**	**tr?**		**tr**								
GP-98-16b	**x**	**x**	**tr?**	**x**	**x**	**x**	**tr**	**tr**				**x**	**x**		**x**	**x**				**x**						
GP-98-17	**x**	**x**		**x**		**x**					**x**		**x**	**x**	**x**		**tr?**			**tr?**	**tr**	**tr?**				
GP-98-18	**x**	**tr?**	**x**	**x**		**x**										**x**		**tr?**		**x**						
GP-98-14	*x*	*x*		*x*		*x*										*x*					*x*					
GP-98-15	*x*	*x*		*x*		*x*										*tr*			*tr?*		*x*					
GP-98-12	**x**	**x**				**x**										**x**	**tr?**			**x**	**x**		**x**			
GP-99-S1A	x	x	x	x		x						x				x				x			x			
GP-99-S1B	*x*	*x*		*x*		*x*										*x*				*x*	*tr*					
GP-99-S1C	x	x	x	x		x						x				x				x			x			
GP-99-A1	x	x		x	x	x		tr					tr			x	x				x	x		x		
GP-99-A2	x	x		x	x	x										x	x			x	x	x		x		
GP-99-A3	x	x		tr	x	x										x	x			x	x	x		x		x
GP-99-A4	x	x		x	x	x											x			tr	x	x		x		
GP-99-E1	x	x			x	x						x	x			x				x			x			
GP-99-E2	x	x			x	x						x	x			x				x			x			
GP-99-E3	x	x			x	x						x	x			x				x			x			
GP-98-19	*x*	*x*		*x*		*x*			*tr*												*x*					
GP-98-20	*x*	*x*		*x*				*tr*		*x*							*x*	*x*		*tr?*	*tr?*					
GP-98-21	x	x	x	x		x										x				x					tr	
GP-98-22	x	x		x		x				tr?						x		x		x	x	x				

Clastic and carbonatic metasediments are indicated in italics, metatuffites and metatuffs in normal, and massive intrusive or lava rocks of basic composition in bold letters.
Abbreviations of mineral names after BUCHER & FREY (1994); [1] = properly: illite – dioctahedral white K-mica; * = ankerite; Sm = smectite; Chl/Sm = chlorite/smectite; Ill/Sm = illite/smectite mixed layers; tr = traces (if phyllosilicate, detectable mostly in the the <2 μm fraction); ? = questionable.

Applying the least-squares method, the calibration was done by regression equations so that the IC boundaries of the anchizone correspond exactly to 0.25 and 0.42°Δ2Θ. Consequently, the actual boundary range of ChC(001) and ChC(002) of the present paper, which correspond to Kübler's original anchizone are 0.26–0.38 and 0.24–0.30° Δ2Θ for fine-clastic metasedimentary rocks, as transformed accordingly from the data of ÁRKAI et al. (1995b).

Electron microprobe (EMP) technique was used for the determination of chemical compositions of rock forming metamorphic minerals. EMP analyses were carried out with a JEOL JCXA-733 instrument equipped with three wavelength-dispersive X-ray spectrometers, using the ZAF correction method. Measuring conditions, standards and errors of quantitative analyses were the same as given by ÁRKAI & SADEK GHABRIAL (1997). Cation numbers per unit cells of the various minerals were calculated in the usual, conventional way.

Major element compositions of bulk rock samples were determined using a Perkin Elmer 5000 atomic absorption spectrophotometer (AAS), after digestion with lithium metaborate. In addition to AAS, permanganometric (FeO), gravimetric (SiO_2, TiO_2, H_2O and P_2O_5) and volumetric (CO_2) methods were applied.

4. Results

Modal and Bulk Rock Compositions

Tab. 2 contains the modal composition of rock samples involved in the present study. Most of the metasedimentary rocks are built up by mineral assemblages consisting of quartz, illite-white K-mica ± chlorite, albite, carbonate minerals (mainly calcite, subordinately dolomite). Accessories are represented by hematite and rutile. Small amounts of goethite accompanied by smectite and mixed-layers refer to post-metamorphic surficial weathering, while the kaolinite+siderite assemblage of sample GP-98-20 may be the result of low-T hydrothermal alteration.

By contrast, metatuffites show more variable modal compositions than metasediments. Metatuffites of the Flösserkogel Fm. (samples GP-98-2-5) are characterized by the presence of K-feldspar and lack of chlorite, in addition to the commonly occurring quartz and illite-white K-mica and eventually occurring albite, dolomite, hematite and calcite. Metatuffites of the Kehr-Vulkanit Fm. (samples GP-98-9-11) are built up by quartz, illite-muscovite, chlorite, calcite, hematite ± albite, ankerite, siderite, rutile and apatite. Metatuffites from the Taschen-Schiefer Fm. (Schöckel nappe, samples GP-99-S1A and C) are charac-

Table 3.
Major element bulk chemical compositions (weight-%).

Sample	SiO_2	TiO_2	Al_2O_3	Fe_2O_3	FeO	MnO	MgO	CaO	Na_2O	K_2O	+H2O	-H2O	CO_2	P_2O_5	total
GP-98-2	54.62	1.06	21.41	3.17	0.66	0.01	2.52	0.39	0.09	12.19	3.31	0.04	0.00	0.43	99.90
GP-98-7	*14.41*	*0.15*	*3.09*	*1.35*	*1.36*	*0.20*	*0.67*	*43.01*	*0.16*	*0.54*	*4.56*	*0.13*	*29.83*	*0.04*	*99.50*
GP-98-9	35.92	4.81	18.82	2.29	9.33	0.14	3.17	7.55	0.30	3.72	5.20	0.07	6.73	1.35	99.40
GP-98-10	29.60	3.81	15.17	2.48	11.35	0.25	3.43	12.33	0.20	2.35	4.68	0.03	12.76	1.01	99.45
GP-98-11	37.40	2.75	12.64	3.04	8.54	0.12	9.66	10.25	0.17	0.10	6.99	0.14	7.28	0.34	99.42
GP-98-13	**45.20**	**4.18**	**13.89**	**6.74**	**6.38**	**0.22**	**5.87**	**8.30**	**3.30**	**0.88**	**3.01**	**0.16**	**0.89**	**0.43**	**99.45**
GP-9-16/a	**47.91**	**3.87**	**16.44**	**3.45**	**8.05**	**0.10**	**4.53**	**3.72**	**3.14**	**3.99**	**3.73**	**0.12**	**0.39**	**0.54**	**99.98**
GP-98-16/b	**47.49**	**3.12**	**13.88**	**6.63**	**6.88**	**0.18**	**5.87**	**4.57**	**3.44**	**2.74**	**3.36**	**0.10**	**0.78**	**0.39**	**99.43**
GP-98-17	**47.39**	**3.56**	**15.42**	**2.45**	**8.42**	**0.17**	**6.06**	**6.22**	**4.09**	**1.35**	**3.76**	**0.06**	**0.23**	**0.34**	**99.52**
GP-98-18	**48.79**	**3.05**	**14.44**	**6.55**	**3.42**	**0.05**	**2.29**	**5.58**	**0.41**	**7.58**	**3.52**	**0.18**	**2.96**	**0.60**	**99.42**
GP-98-15	*53.10*	*1.08*	*20.59*	*2.61*	*6.37*	*0.03*	*3.29*	*0.75*	*1.45*	*4.24*	*5.35*	*0.29*	*0.27*	*0.17*	*99.59*
GP-98-12	**44.08**	**2.66**	**12.09**	**4.54**	**7.28**	**0.17**	**6.29**	**9.74**	**2.33**	**0.02**	**5.13**	**0.10**	**5.07**	**0.19**	**99.69**
GP-99-S1A	50.26	2.56	13.49	2.95	7.57	0.13	6.84	6.83	3.51	1.67	3.56	0.08	0.03	0.39	99.87
GP-99-S1B	*40.41*	*2.91*	*11.88*	*3.86*	*5.30*	*0.27*	*3.58*	*13.22*	*4.42*	*0.79*	*2.98*	*0.37*	*8.84*	*1.03*	*99.86*
GP-99-S1C	49.25	2.44	13.13	3.15	7.50	0.15	8.13	7.32	3.08	1.79	3.34	0.06	0.23	0.32	99.89
GP-99-E1	51.76	2.40	14.35	2.54	7.26	0.14	5.16	7.79	3.49	2.25	2.33	0.12	-	0.39	99.98
GP-99-E2	50.85	2.40	14.94	3.18	6.79	0.15	4.85	8.65	4.01	1.29	2.33	0.10	0.03	0.39	99.96
GP-99-E3	50.98	2.37	14.53	3.14	7.21	0.15	5.27	7.61	3.54	1.79	2.61	0.02	0.26	0.38	99.86
GP-99-A1	36.42	3.34	10.70	2.41	8.25	0.17	6.87	13.28	1.81	2.12	4.67	0.10	9.26	0.38	99.78
GP-99-A2	36.09	3.81	15.36	3.53	10.94	0.13	11.13	4.48	1.03	2.92	6.21	0.09	3.59	0.49	99.80
GP-99-A3	39.23	3.57	14.54	2.17	12.21	0.14	11.13	3.53	1.60	1.96	6.32	0.13	2.94	0.47	99.94
GP-99-A4	39.15	4.30	14.16	3.12	12.08	0.09	10.11	3.26	0.91	2.41	6.45	0.11	3.01	0.81	99.97
GP-98-19	*81.06*	*0.55*	*9.29*	*2.49*	*0.52*	*0.03*	*0.31*	*0.04*	*0.70*	*2.35*	*1.98*	*0.09*	*0.04*	*0.08*	*99.53*
GP-98-21	38.63	4.38	16.34	2.63	10.31	0.10	4.40	7.04	3.22	1.32	5.38	0.11	4.92	0.74	99.52
GP-98-22	43.41	3.16	13.69	1.85	5.11	0.14	1.84	11.49	2.12	2.81	2.98	0.07	10.10	0.56	99.33

Clastic and carbonatic metasedimentary rocks are indicated in italics, metatuffites and metatuffs in normal, and massive intrusive and lava rocks of basic composition in bold letters.

terized by quartz, albite, K-feldspar, illite-white K-mica, chlorite, calcite, actinolite, hematite and titanite. In metatuffites of the Schönberg Fm. of the Schöckel nappe the general appearance of biotite seems to be a distinguishing feature. In the Arzberg locality (samples GP-99-A1-A4) common occurrences of dolomite, calcite, hematite, rutile, ilmenite and apatite, and sporadic occurrences of epidote and tourmaline, whereas in the Silberberg locality (samples GP-99-E1-E3) the lack of white K-mica and the common occurrences of actinolite, epidote, calcite, hematite and titanite are characteristic. In the greenschists of the Sausal Paleozoic (samples GP-98-21 and 22) again the assemblage of quartz, albite, white K-mica, chlorite, calcite and hematite is found, locally with sporadic K-feldspar, rutile and ilmenite. Goethite refers to weathering, while minor amounts of kaolinite and siderite presumably refer to low-T hydrothermal activity.

Considering the metabasic massive rocks of lava or intrusive origin, clinopyroxene is the only relic magmatic mineral (Tab. 2). The metamorphic minerals of the metabasalt from the Kehr-Vulkanit Fm. of the Rannach nappe (sample GP-98-13) consist of quartz, albite, white K-mica, chlorite, actinolite, epidote and dolomite. Other minerals such as prehnite, calcite, siderite, hematite, rutile and titanite occur only as traces. Similar assemblages are found also in the metabasalt and -gabbro samples of the Tyrnaueralm Fm. (Hochlantsch nappe, samples GP-98-16a,b, 17 and 18). In some of them K-feldspar, biotite and pumpellyite also occur. The metabasalt sample GP-98-12 from the Taschen-Schiefer Fm. of the Schöckel nappe from the village Waldstein is built up by quartz, albite, chlorite, calcite, hematite, rutile and titanite, with traces of dolomite.

Major element bulk chemical compositions of representative samples are given in Tab. 3. Their evaluations can be found in context with mineral chemistry in the part “Discussion”.

Illite and Chlorite Crystallinity Indices

Calibrated IC and ChC values are given in Tab. 4. IC values of marly slate and metatuffites from the Flösserkogel Fm. (samples GP-98-1 and 2-5, respectively) prove higher anchizonal conditions. There is no systematic difference between the IC values of slate, marly slate and metatuffites of the Kehr-Vulkanit Fm (samples GP-98-6-11), all referring to boundary conditions between the anchi- and epizones. Disregarding sample GP-98-11 that has anom-

Table 4.
Corrected chlorite and illite crystallinity values measured on <2µm fraction, sedimented mounts (values in Δ°2Θ, CuKα).

Sample	[ChC(001)] ca. 14-Å reflection				[ChC(002)] ca. 7-Å reflection				IC ca. 10-Å	
	AD	EG	Mg, AD	Mg, EG	AD	EG	Mg, AD	Mg, EG	AD	EG
GP-98-1	-	-	-	-	-	-	-	-	*0.318*	*0.252*
GP-98-2	-	-	-	-	-	-	-	-	0.246	0.239
GP-98-3	-	-	-	-	-	-	-	-	0.260	0.292
GP-98-4	-	-	-	-	-	-	-	-	0.279	0.278
GP-98-5	-	-	-	-	-	-	-	-	0.329	0.313
GP-98-6	*0.284*	-	*0.297*	*0.259*	*0.272*	*0.255*	*0.265*	*0.258*	*0.262*	*0.239*
GP-98-7	*0.246*	*0.250*	*0.280*	*0.259*	*0.246*	*0.279*	*0.259*	*0.252*	*0.240*	*0.253*
GP-98-8	-	-	-	-	-	-	-	-	*0.239*	*0 224*
GP-98-9	0.272	0.242	0.284	0.265	0.254	0.236	0.253	0.237	0.259	0.235
GP-98-10	0.255	0.229	0.280	0.269	0.234	0.225	0.243	0.244	0.244	0.233
GP-98-11	0.317	0.299	0.279	0.295	0.303	0.282	0.253	0.273	-	-
GP-98-13	**0.458**	**0.349**	**0.343**	**0.332**	**0.376**	**0.310**	**0.283**	**0.285**	**0.445**	**0.317**
GP-98-16a	**0.384**	**0.428**	**0.367**	**0.356**	**0.302**	**0.341**	**0.282**	**0.291**	**0.528**	**0.432**
GP-98-16b	**0.388**	**0.370**	**0.338**	**0.353**	**0.289**	**0.323**	**0.260**	**0.267**	**0.633**	**0.455**
GP-98-17	**0.290**	**0.355**	**0.292**	**0.308**	**0.279**	**0.305**	**0.270**	**0.272**	**0.503**	**0.469**
GP-98-18	**-**	**-**	**-**	**-**	**0 322**	**0 328**	**-**	**-**	**0.387**	**0 370**
GP-98-14	*0.302*	*0.286*	*0.290*	*0.266*	*0.279*	*0.282*	*0.265*	*0.248*	*0.278*	*0.256*
GP-98-15	*0.303*	*0.313*	*0.279*	*0.260*	*0.280*	*0.300*	*0.264*	*0.257*	*0.282*	*0.287*
GP-98-12	**0.344**	**0.268**	**0.280**	**0.281**	**0.315**	**0.242**	**0.254**	**0.265**	**-**	**-**
GP-99-S1A	0.262	0.261	0.280	0.282	0.242	0.257	0.254	0.244	0.477	0.331
GP-99-S1B	*0.286*	*0.282*	*0.279*	*0.291*	*0.257*	*0.264*	*0.262*	*0.267*	*0.269*	*0.241*
GP-99-S1C	0.235	0.231	0.288	0.260	0.234	0.235	0.266	0.240	0.381	0.317
GP-99-A1	0.275	0.280	0.295	0.283	0.253	0.268	0.261	0.254	-	
GP-99-A2	0.240	0.247	0.277	0.281	0.249	0.242	0.257	0.254	-	
GP-99-A3	0.243	0.243	0.279	0.279	0.242	0.249	0.261	0.259	-	
GP-99-A4	0.260	0.273	0.310	0.317	0.268	0.270	0.288	0.280	-	
GP-99-E1	0.341	0.301	-	0.362	0.280	0.267	0.286	0.284	-	
GP-99-E2	0.255	0.229	0.301	0.349	0.242	0.249	0.241	0.244	-	
GP-99-E3	0.333	0.261	0.400	0.380	0.253	0.256	0.275	0.240	-	
GP-98-19	-	-	-	-	*0 320*	*0 271*	-	-	*0.321*	*0.266*
GP-98-20	-	-	-	-	-	-	-	-	*0.250*	*0.279*
GP-98-21	0.218	0.222	0.262	0.279	0.237	0.230	0.250	0.264	0.256	0.240
GP-98-22	0.234	0.221	0.262	0.256	0.247	0.233	0.247	0.237	0.267	0.248

FWHM measured on AD = air-dried; EG = ethylene-glycol-solvated; Mg,AD = $MgCi_2$-saturated and air-dried; Mg,EG = $MgCi_2$-saturated and ethylene-glycolated mounts.
Clastic and carbonatic rocks are indicated in italics, metatuffites and metatuffs in normal and massive intrusive and lava rocks of basic composition in bold letters.

alously high ChC values [ChC(001) referring to medium-T anchizone, ChC(002) to anchizone/diagenetic zone transition], ChC averages of the slate and metatuffite samples unequivocally show transitional anchi-/epizonal boundary conditions, agreeing fairly well with the IC averages. The pelitic-marly slates of the Kogler Fm., Kalkschiefer nappe (samples GP-98-14 and 15) display higher anchizonal IC and ChC values. The single IC value from the slate of the Taschen-Schiefer Fm., Schöckel nappe (sample GP-99-S1B) also refers to high-T anchizonal metamorphism, while IC values of metatuffites from the same locality (Silberberg, GP-99-S1A and S1C) are significantly higher and apparently correspond only to low-T anchi- or diagenetic zones. By contrast, opposite behaviour of ChC indices can be observed, the ChC values of the metapelite sample referring to higher-grade anchizonal, while those of the metatuffites mostly to epizonal conditions.

Because of the presence of biotite, only the ChC values can be used for evaluating the metatuffites from the Schönberg Fm. (Schöckel Nappe, localities at Arzberg). In sample group GP-99-A1-A4 mean values of ChC(001),AD and ChC(002),AD indicate metamorphism very near to the boundary between the anchi- and epizones. In sample group GP-99-E1-E3 the ChC averages correspond to high-T anchizonal conditions.

IC value of the quartz phyllite sample from the Semriach Phyllite Fm. (Schöckel nappe, GP-98-19) falls within the high-T part of the anchizone, while ChC(002) refers only to the diagenetic zone.

A single IC value from the phyllite of Sausal Paleozoic (GP-98-20) falls to the boundary between the anchi- and epizones. Greenschist samples of the Sausal Paleozoic (samples GP-98-21, 22) show high-T anchizonal IC and mostly epizonal ChC values.

Considering the massive (lava or intrusive) metabasic rocks, their IC and ChC values are strongly varying. IC indices of the metabasalts from the Kehr-Vulkanit Fm. (Rannach nappe, sample GP-98-13) and from the Tyrnaueralm Fm. (Hochlantsch nappe) fall mostly to the diagenetic zone, subordinately to the lower-grade anchizone. Similar conclusions can be drawn from the ChC indices of these rocks. Metabasalt from the Taschen-Schiefer Fm. (Schöckel nappe, sample GP-98-12) displays lower anchizonal-diagenetic ChC indices.

Mineral Chemistry

Chemistries of relic magmatic clinopyroxene and main metamorphic minerals were determined by EMP. Out of these results, the data of dioctahedral white K-micas (Tab. 5) and chlorites (Tab. 6) are summarized here. The evaluation of mineral chemistries are given in the part "Discussion" in context to the phyllosilicate evolution.

5. Discussion

As usual, the common modal compositions of pelitic-marly metasediments studied have no diagnostic value for evaluating metamorphic grade. The same is valid also for the majority of the meta-tuffites. The actinolite + epidote + biotite + chlorite assemblage from the Schönberg Fm. (Schöckel nappe, Arzberg, samples GP-99-E1-E3) may refer to low-T greenschist facies conditions (see BUCHER & FREY, 1994). Biotite is found also in an other locality of

Table 5.
Average chemical compositions of white K-micas (weight-% and cation numbers) determined by EMP.

sample GP-	98-7	98-9	98-10	98-11	98-13	98-16a	98-17	98-15	98-19	98-22	99-A1	99-A2	99-A4
n	1	6	5	3	4	6	3	3	3	6	3	3	3
SiO_2	48.75	45.57	46.75	48.99	46.96	50.18	49.35	48.84	48.12	48.62	46.53	49.50	48.08
TiO_2	0.19	0.22	0.14	0.11	0.12	0.08	0.02	0.39	0.22	0.47	0.62	0.85	0.66
Al_2O_3	38.53	37.01	36.13	33.99	28.05	26.50	27.05	33.71	37.26	28.31	30.89	27.67	28.31
*FeO	0.89	1.09	1.45	2.47	5.46	5.78	6.87	2.03	1.21	4.23	4.51	6.05	5.18
MnO	0.01	0.02	0.02	0.01	0.03	0.05	0.03	0.02	0.00	0.01	0.00	0.03	0.01
MgO	0.57	0.85	0.98	1.39	2.10	2.70	1.57	1.81	0.67	2.55	2.13	4.07	2.92
CaO	0.06	0.06	0.08	0.04	0.13	0.03	0.12	0.03	0.01	0.03	0.02	0.04	0.01
Na_2O	0.42	0.69	0.47	0.32	0.22	0.09	0.04	0.39	0.58	0.07	0.26	0.08	0.22
K_2O	8.77	9.30	9.24	10.50	9.78	9.20	9.82	9.34	9.41	9.71	10.45	10.30	10.55
total	98.19	94.81	95.26	97.82	92.84	94.61	94.87	96.56	97.48	94.00	95.41	98.59	95.94
number of cations on the basis of 22 oxygens													
Si	6.18	6.05	6.17	6.36	6.53	6.81	6.74	6.37	6.19	6.62	6.30	6.52	6.50
Al^{IV}	1.82	1.95	1.83	1.64	1.47	1.20	1.26	1.63	1.81	1.39	1.70	1.48	1.50
Al^{VI}	3.94	3.84	3.79	3.56	3.14	3.04	3.09	3.55	3.84	3.16	3.23	2.81	3.01
Ti	0.02	0.02	0.01	0.01	0.01	0.09	0.00	0.04	0.02	0.05	0.06	0.08	0.07
$*Fe^{2+}$	0.09	0.12	0.16	0.27	0.64	0.66	0.78	0.22	0.13	0.48	0.51	0.67	0.59
Mn	0.00	0.00	0.00	0.00	0.00	0.01	0.00	0.00	0.00	0.00	0.00	0.00	0.00
Mg	0.11	0.17	0.19	0.27	0.44	0.55	0.32	0.35	0.13	0.52	0.43	0.79	0.59
sum R^{VI}	4.16	4.18	4.16	4.11	4.23	4.26	4.20	4.17	4.12	4.21	4.23	4.35	4.25
Ca	0.01	0.01	0.01	0.01	0.02	0.00	0.02	0.00	0.00	0.00	0.00	0.01	0.00
Na	0.10	0.18	0.12	0.08	0.06	0.02	0.01	0.10	0.15	0.02	0.07	0.02	0.06
K	1.42	1.58	1.56	1.74	1.74	1.59	1.71	1.56	1.54	1.69	1.80	1.73	1.82
t.i.c.	1.54	1.77	1.70	1.83	1.84	1.62	1.76	1.66	1.69	1.71	1.88	1.76	1.88
total	13.69	13.94	13.84	13.94	14.05	13.88	13.94	13.83	13.81	13.92	14.11	14.11	14.13
XMg	0.03	0.04	0.05	0.07	0.10	0.13	0.08	0.09	0.03	0.12	0.10	0.18	0.14
$Fe^{2+}/(Fe^{2+}+Mg)$	0.47	0.42	0.45	0.50	0.59	0.55	0.72	0.39	0.50	0.48	0.55	0.46	0.50
$Al^{VI}/(Al^{VI}+Fe^{2+}+Mg)$	0.95	0.93	0.91	0.87	0.74	0.72	0.74	0.86	0.94	0.76	0.77	0.66	0.72
Na/(Na+K)	0.07	0.10	0.06	0.05	0.04	0.02	0.01	0.06	0.09	0.01	0.04	0.01	0.03

* = total Fe calculated as FeO and Fe^{2+}, respectively; t.i.c. = total interlayer charge; n = number of measurements.

Table 6.
Average chemical compositions of chlorite determined by EMP (weight-% of oxides and cation numbers on the basis of 28 oxygens).

sample GP-	98-7	98-9	98-10	98-11	98-13	98-16a	98-16b	98-17	98-18	98-15	98-12	98-22	99-S1A	99-S1B	99-S1C	99-A1	99-A2	99-A3	99-A4	99-E1	99-E2	99-E3
n	4	4	4	3	9	4	6	5	4	4	11	6	9	4	3	6	3	3	4	10	3	3
SiO_2	24.46	24.45	23.22	28.91	26.24	29.38	26.41	27.19	26.24	25.59	27.05	25.01	27.94	26.52	27.64	2.55	27.48	27.24	26.78	26.95	25.61	25.58
TiO_2	0.04	0.13	0.06	0.04	0.05	0.05	0.05	0.03	0.03	0.06	0.07	0.12	0.09	0.17	0.00	0.03	0.17	0.12	0.10	0.05	0.09	0.05
Al_2O_3	24.39	24.21	23.57	19.48	18.40	18.45	18.65	18.57	18.97	22.67	20.43	21.18	19.35	19.1	19.92	20.84	21.27	21.09	21.15	19.90	21.52	20.86
*FeO	32.66	32.24	33.89	21.06	23.13	23.04	27.24	26.48	28.04	30.26	21.90	30.99	24.26	24.9	23.21	22.46	20.68	21.14	22.49	26.47	26.41	24.74
MnO	0.04	0.05	0.04	0.07	0.37	0.42	0.29	0.21	0.09	0.05	0.25	0.08	0.30	0.21	0.33	0.07	0.12	0.14	0.08	0.39	0.45	0.38
MgO	8.69	8.68	7.69	20.33	17.94	17.20	15.54	15.54	14.30	11.29	18.48	11.30	16.59	17.28	18.34	17.91	19.53	19.35	17.99	15.27	14.73	15.89
CaO	0.05	0.02	0.03	0.10	0.09	0.09	0.04	0.16	0.06	0.04	0.06	0.06	0.21	0.02	0.02	0.04	0.02	0.09	0.01	0.06	0.01	0.00
Na_2O	0.01	0.01	0.00	0.01	0.02	0.01	0.00	0.00	0.00	0.02	0.01	0.01	0.04	0.02	0.00	0.02	0.01	0.13	0.00	0.05	0.01	0.01
K_2O	0.01	0.19	0.00	0.03	0.02	0.62	0.28	0.01	0.01	0.06	0.01	0.03	0.09	0.01	0.00	0.03	0.04	0.05	0.00	0.04	0.08	0.00
total	90.35	89.98	88.50	90.03	86.27	89.26	88.50	88.19	87.74	90.04	88.23	88.78	88.89	88.23	89.45	86.86	89.34	89.34	88.58	89.14	88.90	87.50
Si	5.17	5.19	5.08	5.76	5.58	5.99	5.59	5.73	5.61	5.36	5.55	5.36	5.76	5.55	5.63	5.34	5.52	5.49	5.48	5.61	5.36	5.39
Al^{IV}	2.83	2.81	2.92	2.24	2.42	2.01	2.41	2.27	2.39	2.64	2.45	2.64	2.24	2.45	2.37	2.66	2.48	2.51	2.52	2.39	2.64	2.61
Al^t	6.08	6.05	6.07	4.58	4.62	4.44	4.65	4.61	4.78	5.60	4.94	5.35	4.71	4.71	4.78	5.15	5.04	5.01	5.10	4.88	5.31	5.18
Al^{VI}	3.25	3.24	3.15	2.34	2.20	2.43	2.24	2.34	2.39	2.96	2.49	2.72	2.46	2.26	2.41	2.50	2.56	2.51	2.59	2.50	2.66	2.58
Ti	0.01	0.02	0.01	0.01	0.01	0.01	0.01	0.01	0.01	0.01	0.01	0.02	0.01	0.03	0.00	0.01	0.03	0.02	0.02	0.01	0.01	0.01
$*Fe^{2+}$	5.78	5.72	6.20	3.51	4.12	3.94	4.83	4.67	5.02	5.30	3.76	5.56	4.18	4.36	3.95	3.94	3.47	3.57	3.85	4.61	4.62	4.36
Mg	2.74	2.75	2.51	6.04	5.69	5.24	4.91	4.88	4.56	3.53	5.66	3.61	5.10	5.39	5.57	5.61	5.85	5.82	5.49	4.74	4.59	5.00
Mn	0.01	0.01	0.01	0.01	0.07	0.07	0.05	0.04	0.02	0.01	0.04	0.01	0.06	0.04	0.06	0.01	0.02	0.02	0.01	0.07	0.08	0.07
sum R^{VI}	11.77	11.74	11.87	11.91	12.08	11.68	12.03	11.93	11.98	11.81	11.96	11.92	11.82	12.07	11.98	12.06	11.92	11.93	11.96	11.92	11.97	12.01
Ca	0.01	0.00	0.01	0.02	0.02	0.02	0.01	0.04	0.01	0.01	0.01	0.01	0.05	0.01	0.01	0.01	0.00	0.02	0.00	0.01	0.00	0.00
Na	0.00	0.00	0.00	0.00	0.01	0.00	0.00	0.00	0.00	0.01	0.00	0.00	0.02	0.01	0.00	0.01	0.01	0.05	0.00	0.00	0.01	0.00
K	0.00	0.05	0.00	0.01	0.01	0.16	0.07	0.00	0.00	0.02	0.00	0.01	0.02	0.00	0.00	0.01	0.01	0.01	0.00	0.01	0.02	0.00
sum(Ca+Na+K)	0.02	0.06	0.01	0.03	0.03	0.18	0.08	0.04	0.02	0.03	0.02	0.03	0.08	0.01	0.01	0.02	0.02	0.08	0.00	0.03	0.02	0.00
total	19.79	19.79	19.88	19.95	20.11	19.86	20.11	19.97	20.00	19.84	19.99	19.95	19.90	20.08	19.99	20.08	19.95	20.01	19.96	19.95	20.02	20.02
XMg	0.23	0.23	0.21	0.51	0.47	0.45	0.41	0.41	0.38	0.30	0.47	0.30	0.43	0.45	0.46	0.47	0.49	0.49	0.46	0.40	0.38	0.42
$Fe^{2+}/(Fe^{2+}+Mg)$	0.68	0.68	0.71	0.37	0.42	0.43	0.50	0.49	0.52	0.60	0.40	0.61	0.45	0.45	0.42	0.41	0.37	0.38	0.41	0.49	0.50	0.47
$Si/(Si+Al^t)$	0.46	0.46	0.46	0.56	0.55	0.58	0.55	0.55	0.54	0.49	0.53	0.50	0.55	0.54	0.54	0.51	0.52	0.52	0.52	0.54	0.50	0.51
$Si+Al^t+Mg+Fe^{2+}$	19.76	19.71	19.85	19.90	20.00	19.60	19.97	19.88	19.96	19.79	19.90	19.89	19.75	19.99	19.92	20.04	19.88	19.89	19.93	19.85	19.88	19.94
$Al^t+Mg+Fe^{2+}$	14.59	14.52	14.78	14.13	14.42	13.61	14.38	14.16	14.35	14.43	14.36	14.52	13.99	14.45	14.30	14.70	14.36	14.40	14.44	14.24	14.52	14.54

Total Fe is calculated as FeO and Fe^{2+} respectively.
n = number of analyses.

Arzberg (GP-99-A1-4), actinolite also from the Taschen-Schiefer Fm (Silberberg, GP-99-S1A and C), implying higher-grade (presumably greenschist facies) conditions. However, biotite may form by reactions involving K-feldspar that is frequently present in the studied samples, at significantly lower temperatures than by the classic reaction of metapelite involving chlorite and muscovite (Winkler, 1979; Bucher & Frey, 1994; see also Árkai et al., 1995a).

The metamorphic mineral assemblages of metabasalts and metagabbro containing chlorite, actinolite, epidote and prehnite or epidote, pumpellyite and prehnite refer to either transitional subgreenschist/greenschist facies conditions or to crystallization under disequilibrium conditions characterized by de-creasing temperature. Out of these possibilities the latter seems to be much more plausible (see also the evaluation of IC and ChC data).

It is obvious from the results above that no overall valid relations can be deduced when comparing the IC and ChC values of various lithotypes found in the same outcrop. There are certain localities (e.g., GP-98-1-5; GP-98-6-11) where the IC values of the associated metapelites and metatuffites are in agreement with each other and also with the ChC values. In general, ChC indices can be used for approximate determination of metamorphic zones in both lithotypes.

By contrast, IC of basic metatuffites behaves anomalously in some other localities, (e.g., GP-99-S1A and C; GP-98-21 and 22). In these localities metatuffites show anoma-

lously high IC values, indicating anomalously low apparent grade, as compared to IC values of the associated metapelites. However, ChC indices proved to be reliable metamorphic zone indicators in both lithotypes also in these localities.

As compared to the mineral assemblages, anomalously high IC and ChC values were obtained from the massive metabasic rocks. In addition to bulk rock and mineral chemical effects outlined below, the lower porosity and permeability of these rocks as compared to metatuffites may be a cause responsible for the retarded reaction progress of phyllosilicates (see also SCHMIDT & ROBINSON, 1997).

In order to evaluate the metamorphic zone-indicating significance of IC and ChC measured in various lithotypes, eventual effects of factors that may affect the FWHM values of basal reflections of illite and chlorite are discussed below.

Factors Affecting Illite Crystallinity

Text-Fig. 4 demonstrates that the differences between IC values measured on airdry and glycolated mounts decrease with decreasing IC,AD, i.e., with increasing grade or temperature. The strong positive linear correlation implies that the amounts of swelling (smectitic) mixed-layers, being responsible for the sharpening of the 10-Å reflection after glycolation, decrease with advancing grade. This trend corresponds to the general evolution path of illite-muscovite in diagenetic and incipient metamorphic conditions (for summary reviews see FREY, 1987; MERRIMAN & PEACOR, 1999). Judging from the relatively low absolute values of the differences, the proportion of swelling component in illite of the <2µm grain-size fraction may be subordinate. It is worth mentioning that glycolation causes small-scale broadening of the 10-Å peak (negative values) in certain epizonal samples.

The trend in Text-Fig. 4 would require an increase in total interlayer charge (t.i.c.) and K with decreasing IC. However, as demonstrated by Tab. 5, both t.i.c. and K content vary within relatively narrow ranges (1.51–1.84 and 1.42-1.74, respectively), showing no systematic differences either between the various lithotypes or in function of IC. [Correlation coefficients between IC,AD and t.i.c (–0.07) and IC,AD and K (0.28) are not significantly differing from zero.]

EMP analyses (summarized in Tab. 5) were done on white mica flakes necessarily larger than the <2µm fraction's grains studied conventionally by XRD. Using microstructural criteria, larger flakes and their aggregates accumulated in the micro-shear cleavage zones were analysed preferentially. Although involvement of detrital mica grains in the EMP analyses can not be ruled out perfectly, the majority of the EMP data has been obtained on newly formed (metamorphic) white micas of larger (>5 µm) grain-size. Thus, compositional trend in function of grain-size of metamorphic white K-micas can be set up in an indirect way, comparing XRD and EMP data. This trend suggests that reaction progress of illite to white K-mica has reached a more advanced stage in the fluid-rich micro-shear (cleavage) zones than that of the small-grained white K-micas found in the matrix. In these shear zones carbonate minerals and quartz also have very often accumulated, in addition to white mica and chlorite.

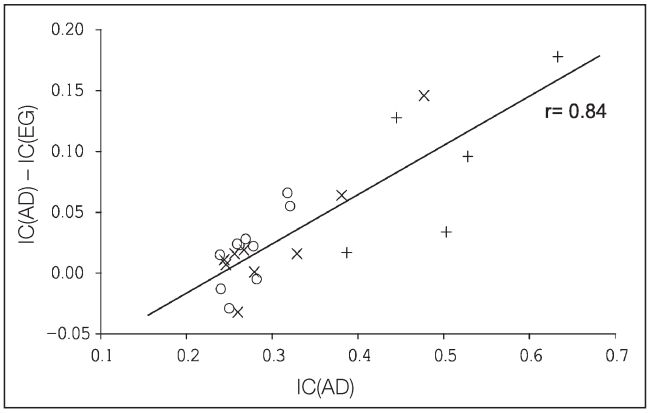

Text-Fig. 4.
Effect of ethylene glycol solvation on illite crystallinity in function of metamorphic grade (IC,AD).
O = metapelite; X = metatuffite; + = massive (lava or intrusive) metabasic rock.

Text-Fig. 5 shows the chemical relations of dioctahedral white K-micas. The subordinate (generally <20 %) pyrophyllite component is a consequence of the t.i.c. deficiency as compared to ideal muscovite or celadonite. There are complete overlaps between the three main rock groups. Metapelites are characterized by Ms>Cel ratios, while the whole range of Ms-Cel solid solution is represented by metatuffites and basic meta-igneous rocks, the latter two rock types having predominantly of celadonitic white K-micas.

At the P = 5 % level significant correlations were found between IC,AD and Cel% (r = 0.59), IC,AD and $Al^{VI}/(Al^{VI}+Fe^{2+}+Mg)$, where r = –0.60, and IC,AD and $Fe^{2+}/(Fe^{2+}+Mg)$, where r = 0.60. The strongest correlation being significant at P = 1 % level was found between IC,AD and Si content (r = 0.77), which is also a function of the proportion of smectitic interlayers, in addition to the dominating role of the celadonite content. One may conclude therefore that both the amounts of smectitic mixed-layers acting mostly in the finer-grained fraction and the celadonite content playing role also in the larger grain population affect the illite crystallinity. With increasing celadonite content the FWHM of the 10-Å reflection increases, thus indicating apparently lower metamorphic grade (temperature). This conclusion confirms the early statement of ESQUEVIN (1969) who has found that IC values of only aluminous illites can be used for indicating metamorphic grade, magnesian illites being unsuitable. ESQUEVIN (1969) used the I5 Å/I10 Å ratio to estimate the

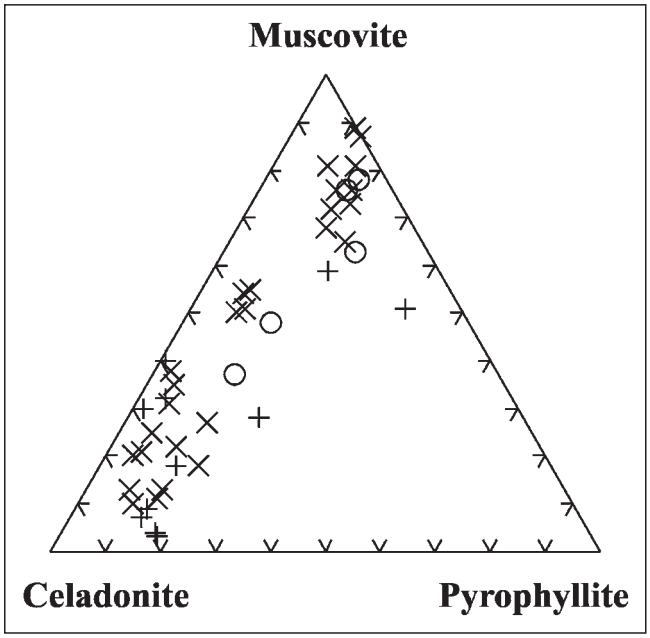

Text-Fig. 5.
Muscovite – celadonite – pyrophyllite end-member relations of dioctahedral white K-micas, calculated from EMP data after VIDAL & PARRA (2000). For symbols see Text-Fig. 4.

Al/Mg relation. However, this intensity ratio proved to be unreliable for estimating chemical relations (HUNZIKER et al., 1986).

At the P = 5 % level significant positive correlations were found between MgO (r = 0.67), FeO (r = 0.42) and FeO_{total} (r = 0.51) contents of bulk rocks and chlorites (see Tables 3 and 5). Out of ratios of major elements, only the $Al_2O_3/(Al_2O_3 + FeO + MgO)$ and $Al_2O_3/(Al_2O_3 + FeO_{total} + MgO)$ ratios of bulk rocks and white micas show moderate (at P = 5 % level significant) positive correlations (r = 0.48 and 0.46, respectively), indicating that the more basic a rock is, the more celadonitic the chemistry of its white K-mica will be. Consequently, IC values obtained on mixed (tuffitic) and meta-igneous rocks of basic composition are larger and indicate apparently lower metamorphic grade than the associated normal pelitic metasedimentary rocks.

Chemical Relations of Chlorite

Similarly to white K-mica, larger flakes and monomineralic aggregates of chlorite commonly found in micro-shear (cleavage) zones, vesicle fillings or in pseudomorphs after magmatic phenocrysts were analysed by EMP. As to Tab. 6, the t.i.c. of chlorites is generally lower than 0.1 p.f.u. (considering 28 oxygens), and reaches 0.2 only in one case.

Consequently, the quantities of smectitic and/or mica-like impurities being present either in form of mixed-layered components or discrete phases should be extremely low. By contrast, the apparent octahedral vacancies abbreviated as □ (supposing tri-trioctahedral structure) range up to c. 0.4 p.f.u., and thus, the proportion of smectitic mixed-layers calculated on the basis of apparent octahedral vacancies using the method of BETTISON & SCHIFFMAN (1988) may reach 15–17 %, however its values commonly range between 0 and 5 %. This contradiction can be solved by a thorough evaluation of EMP data outlined below.

Although t.i.c. of individual chlorite analyses are generally low, only rather few analyses fulfil the strict requirements of VIDAL & PARRA (2000) for selecting correct chemical data on "pure" chlorite. These criteria are as follows:

a) Totals vary between 84 and 91 weight-%;
b) $\Sigma(Na_2O + K_2O + CaO) < 0.5$ weight-% or $(Ca + Na + K) < 0.1$ p.f.u. and
c) $\square = (Al^{VI}-Al^{IV})/2 = 12 - \Sigma R^{VI}$ within an error of ±15 %.

Selecting the appropriate analyses and plotting their end-member relations after VIDAL & PARRA (2000) Text-Fig. 6a shows that the di-trioctahedral (DT, i.e., sudoitic) substitution also plays an important role in addition to the dominant $FeMg_{-1}$ (FM) and Tschermak [TK: $Al^{IV}Al^{VI}Si_{-1}(Mg,Fe)_{-1}$] substitutions in chlorites. The proportion of dioctahedral end-member is usually <10 %, however it may reach 20 %. Thus, apparent octahedral vacancies given in Tab. 6 are mostly plausible consequences of the transient (tri-dioctahedral) nature of the chlorites rather than those of the smectitic or mica-like impurities, the presence of which is not supported by the amounts of alkalis, either. However, when plotting all of the EMP analyses in Text-Fig. 6b, the scatter of the sudoitic substitution increases, indicating that smectitic impurities are also acting in addition to DT substitution. Figs. 6a and 6b show that metapelites have higher "amesite", sudoite (and smectite) contents than metatuffites and metabasites, the latter having higher clinochlore + daphnite contents and generally lower sudoitic substitutions.

Tab. 7 summarizes the statistical parameters of regressions calculated between the chlorite properties. With decreasing total amounts of octahedral divalent cations the Si content also decreases (relation 11 in Tab. 7). This relation displayed in Text-Fig. 7 corresponds to none of the main trends of mixing between chlorite and other minerals displayed by JIANG et al. (1994). Instead, together with relations [1, 4 and 5] this trend refers to TD substitution. The rather weak but at P = 5 or 1% levels significant correlations of relations [6] and [9] in Tab. 7 refer to subordinate contribution of smectitic and/or mica-like impurities to "chlorite" chemistries.

Factors Affecting Chlorite Crystallinity

Figs. 8a and 8b show that glycolation and Mg-saturation affect ChC(001): with increasing FWHM values of the <2μm grain-size airdry mounts the 14-Å peak becomes

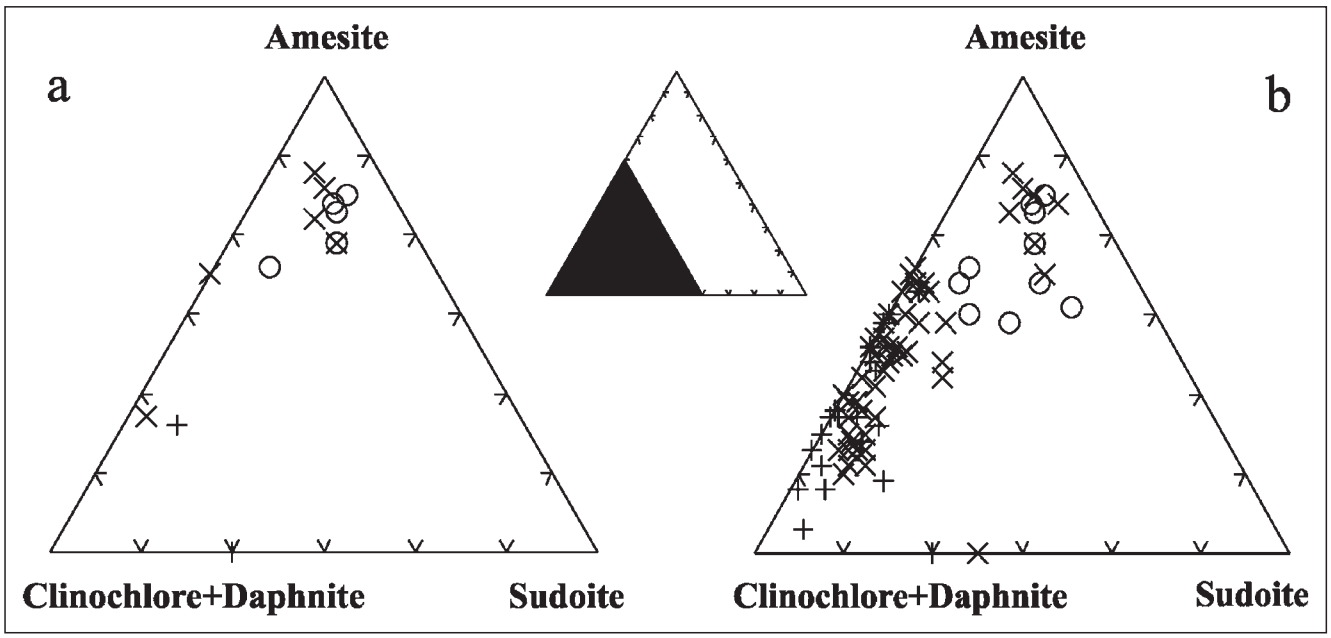

Text-Fig. 6.
End-member relations of chlorite analyses using the criteria of VIDAL & PARRA (2000) for selecting "pure" chlorites (a) and displaying all analyses (b).
End-members are as follows: "amesite": $(Mg,Fe)_8Al_4[Si_4Al_4O_{20}](OH)_{16}$; sudoite: $(Mg,Fe)_4Al_6\square_2[Si_6Al_2O_{20}](OH)_{16}$ and clinochlore + daphnite: $(Mg,Fe)_{10}Al_2[Si_6Al_2O_{20}](OH)_{16}$.
For symbols see Text-Fig. 4.

Table 7.
Correlation coefficients (r) and parameters of linear regressions (y = ax + b) between various chlorite properties.
* = r differs significantly from zero at P = 5 %; ** = at P = 1 % and *** = at P = 0.1 % levels.

relation	y	x	a	b	r	n
1	□	Al^{VI}	0.216	-0.465	0.68***	24
2	□	Al^{IV}	0.072	-0.083	0.14	24
3	□	Al(total)	0.098	-0.405	0.48*	24
4	□	total oct. R^{2+}	-0.199	1.944	-0.80***	24
5	□	Al^{VI}-Al^{IV}	0.464	0.053	0.93***	24
6	t.i.c.	Al^{IV}	-0.112	0.332	-0.49*	24
7	t.i.c.	Al^{VI}	-0.015	0.090	-0.11	24
8	t.i.c.	Al^{VI}-Al^{IV}	0.069	0.044	0.31	24
9	t.i.c.	□	0.256	0.026	0.58**	24
10	Al^{VI}-Al^{IV}	Al(total)	0.257	-1.215	0.63**	24
11	Si	total oct. R^{2+}	0.325	2.476	0.65***	24
12	Al^{IV}	ChC(001), AD	-1.612	2.977	-0.46*	22
13	Al^{IV}	ChC(001), EG	-2.568	3.223	-0.65**	22
14	Al^{IV}	ChC(001), MgEG	-2.202	3.165	-0.40	22
15	Al^{IV}	ChC(001), MgAD	-1.780	3.040	-0.29	21
16	Al^{IV}	ChC(002), AD	-2.804	3.254	-0.45*	22
17	Al^{IV}	ChC(002), EG	-3.652	3.478	-0.55**	22
18	Al^{IV}	ChC(002), MgAD	-7.158	4.382	-0.45*	22
19	Al^{IV}	ChC(002), MgEG	-7.835	4.538	-0.61**	22
20	$Al^{VI}/(Al^{VI}+Fe^{2+}+Mg)$	ChC(001), AD	-0.206	0.279	-0.47*	22
21	$Al^{VI}/(Al^{VI}+Fe^{2+}+Mg)$	ChC(001), EG	-0.199	0.274	-0.42	22
22	$Al^{VI}/(Al^{VI}+Fe^{2+}+Mg)$	ChC(001), MgAD	-0.239	0.292	-0.30	22
23	$Al^{VI}/(Al^{VI}+Fe^{2+}+Mg)$	ChC(001), MgEG	-0.318	0.314	-0.46*	22
24	$Al^{VI}/(Al^{VI}+Fe^{2+}+Mg)$	ChC(002), AD	-0.224	0.282	-0.28	24
25	$Al^{VI}/(Al^{VI}+Fe^{2+}+Mg)$	ChC(002), EG	-0.314	0.305	-0.37	24
26	$Al^{VI}/(Al^{VI}+Fe^{2+}+Mg)$	ChC(002), MgAD	-0.764	0.419	-0.38	22
27	$Al^{VI}/(Al^{VI}+Fe^{2+}+Mg)$	ChC(002), MgEG	-0.820	0.432	-0.51*	22
28	$Fe^{2+}/(Fe^{2+}+Mg)$	ChC(001), AD	-0.478	0.633	-0.28	22
29	$Fe^{2+}/(Fe^{2+}+Mg)$	ChC(001), EG	-0.565	0.652	-0.29	22
30	$Fe^{2+}/(Fe^{2+}+Mg)$	ChC(001), MgAD	-0.595	0.671	-0.19	21
31	$Fe^{2+}/(Fe^{2+}+Mg)$	ChC(001), MgEG	-0.815	0.738	-0.30	22
32	$Fe^{2+}/(Fe^{2+}+Mg)$	ChC(002), AD	-0.591	0.662	-0.20	24
33	$Fe^{2+}/(Fe^{2+}+Mg)$	ChC(002), EG	-0.560	0.652	-0.18	24
34	$Fe^{2+}/(Fe^{2+}+Mg)$	ChC(002), MgAD	-2.925	1.260	-0.37	22
35	$Fe^{2+}/(Fe^{2+}+Mg)$	ChC(002), MgEG	-2.861	1.236	-0.45*	22
36	T°C [Cathelineau, 1988]	ChC(001), AD	-234	411	-0.40	22
37	T°C [Cathelineau, 1988]	ChC(001), EG	-411	458	-0.64**	22
38	T°C [Cathelineau, 1988]	ChC(001), MgAD	-276.5	426	-0.27	21
39	T°C [Cathelineau, 1988]	ChC(001), MgEG	-345	446	-0.38	22
40	T°C [Cathelineau, 1988]	ChC(002), AD	-412	453	-0.40	22
41	T°C [Cathelineau, 1988]	ChC(002), EG	-579	497	-0.53*	22
42	T°C [Cathelineau, 1988]	ChC(002), MgAD	-1105	632	-0.42*	22
43	T°C [Cathelineau, 1988]	ChC(002), MgEG	-1184	650	-0.56*	22
44	□	ChC(001), AD	-0.128	0.128	-0.08	22
45	□	ChC(001), EG	0.287	0.011	0.17	22
46	□	ChC(001), MgEG	-0.574	0.263	-0.24	22
47	t.i.c.	ChC(001), AD	0.288	-0.035	0.37	22
48	t.i.c.	ChC(001), EG	0.560	-0.107	0.65**	22
49	t.i.c.	ChC(001), MgAD	0.366	-0.059	0.27	21
50	t.i.c.	ChC(001), MgEG	0.277	-0.033	0.23	22
51	Al^{VI}	ChC(001), AD	-2.404	3.298	-0.48*	22
52	Al^{VI}	ChC(001), EG	-2.750	3.364	-0.49*	22
53	Al^{VI}	ChC(001), MgAD	-2.811	3.437	-0.32	21
54	Al^{VI}	ChC(001), MgEG	-3.713	3.708	-0.47*	22

n = number of data pairs.

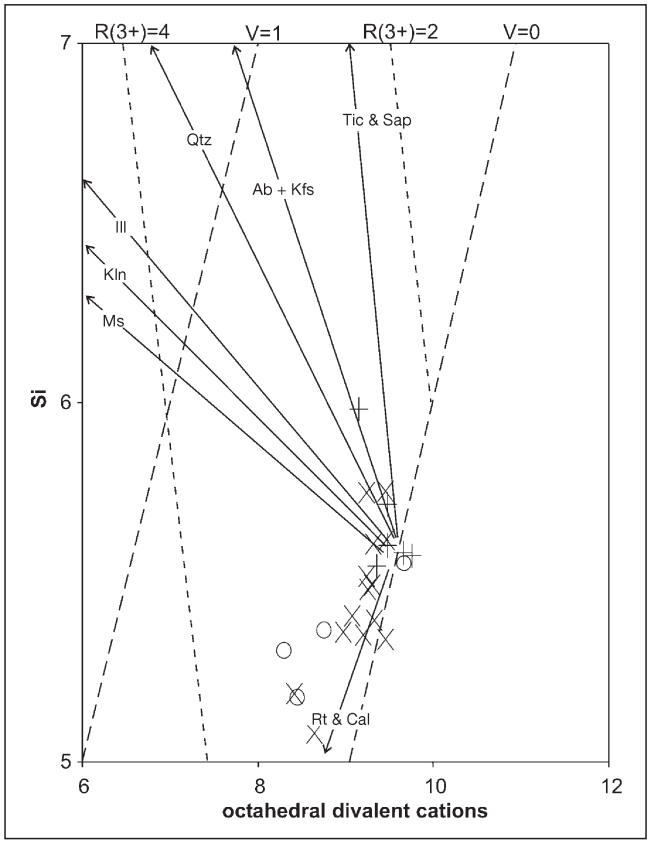

Text-Fig. 7.
Si content of chlorite in function of sum of octahedral divalent cations.
Iso-lines of apparent octahedral vacancies, R^{3+} content and trends of mixing between chlorite and other phases are plotted after JIANG et al. (1994).
Legend as in Text-Fig. 4.

more and more sharp, the effect being more regular at Mg-saturation than at glycolation. Similarly to white K-micas, these trends indicate that swelling mixed-layers are present in the <2μm fraction chlorites in higher quantities than in the larger grains analysed by EMP. The commonly subordinate quantities of smectitic component decrease with increasing grade (i.e., with decreasing FWHM values). In certain cases, especially at epizonal grade Mg-saturation causes small-scale but regular broadening of the 14-Å peak. This effect might be explained either by the formation and existence of high interlayer-charge (rather weakly swelling) vermiculitic mixed-layers and/or by an effect of ethylene glycol and Mg-containing solution loosening and splitting the originally large crystallites into smaller domains along planar structural defects, similarly to that observed in white K-micas.

Conclusions drawn on the role of mixed-layers in anchizonal chlorites from XRD data of the <2μm grain-size fraction mounts are in contradiction with the chemical data of larger chlorite grains studied by EMP. In this respect white K-mica and chlorite are similar and both refer to grain-size and rock microstructure dependent crystal structural and mineral chemical inhomogeneities of these minerals. These inhomogeneities may considerably restrict the validity of the following discussion in which ChC indices are compared to chlorite chemistries.

As summarized in Tab. 7, in general there are no correlations significant at least at P = 5 % level between the ChC values and total interlayer charge [relations 47–50 in Tab. 7] and ChC values and apparent octahedral vacancies [relations 44–46 in Tab. 7]. Moderate, mostly at P = 5 and 1 % levels significant negative correlations exist between ChC and Al^{IV} content [relations 12–19 in Tab. 7]. Rather loose (mostly only at P = 5 % level significant) negative correlations are found between the Al^{VI} content and ChC and between the $Al^{VI}/(Al^{VI}+Fe^{2+}+Mg)$ ratio and ChC [relations 51–54 and 20–27 in Tab. 7], while no significant correlations exist between $Fe^{2+}/(Fe^{2+}+Mg)$ and ChC [relations 28–35 in Tab. 7].

Comparison of ChC indices with chlorite chemistries confirm that chlorite crystallinity reflects the integrated effects of swelling mixed-layers and dioctahedral (sudoitic) substitutions, while the Fe/Mg ratio does not influence ChC. Considering also the mainly insignificant amounts of smectitic impurities, the moderate but mostly significant negative correlations between Al^{IV} and ChC and temperature and ChC [relations 36–42 in Tab. 7] proves that the empirical chlorite-Al^{IV} geothermometer of CATHELINEAU & NIEVA (1985) and CATHELINEAU (1988) and its corrected varieties (KRANIDIOTIS & MACLEAN, 1987; JOWETT, 1991; ZANG & FYFE, 1995) reflects not only the decreasing amounts of smectitic impurities with advancing grade but also a regular change of chemistry of chlorite structure sensu stricto.

When evaluating the metamorphic petrogenetic significance of chlorites, the relations between bulk rock and chlorite chemistries should also be taken into consideration. Because of the great variability of bulk rock chemistries including strongly varying carbonate contents, and because of the polyphase nature of the rocks, the correlations between bulk rock and chlorite chemistries should be necessarily rather weak in general. Thus, no significant correlations were found in SiO_2, Al_2O_3 and $FeO_{(total)}$ amounts and $Al_2O_3/(Al_2O_3+SiO_2)$ ratios between bulk rocks and chlorites. By contrast, significant positive correlations were found for MgO (r = 0.82, P = 0.1%), for MgO/(MgO+FeO) ratio (r = 0.62, P = 1%) and for $Al_2O_3/(Al_2O_3+MgO+FeO_{total})$ ratio (r = 0.44, P = 5%) between bulk rocks and chlorites. Surprisingly similar relations were found by ÁRKAI & SADEK GHABRIAL (1997) between chlorites and their hosting meta-igneous rocks with compositions ranging from basic to acidic.

Thus, combining the bulk rock chemistry – chlorite chemistry – ChC relations, one may conclude that the $Al_2O_3/(Al_2O_3+MgO+FeO_{total})$ ratio of bulk rocks should be taken into account when ChC values and chlorite chemistry (first of all, Al^{IV}) are intended to use for estimating diagenetic and metamorphic zones. An increase in $Al_2O_3/(Al_2O_3+MgO+FeO_{total})$ ratio of bulk rock results in increase in $Al_2O_3/(Al_2O_3+MgO+FeO_{total})$ ratio of chlorite and decrease in ChC indices providing higher apparent metamorphic grades. By contrast, changing $Al_2O_3/(Al_2O_3+SiO_2)$ and $MgO/(MgO+FeO_{total})$ ratios has no remarkable influence on ChC.

6. Conclusions

Evaluating illite and chlorite crystallinity, mineral and bulk rock chemical data obtained from metatuffites and meta-igneous rocks of basic to intermediate compositions and pelitic-marly metasediments all deriving from the Graz and Sausal Paleozoic of the Eastern Alps, the following conclusions are drawn.

1) In general, chlorite crystallinity indices can be used for approximate determination of diagenetic and metamorphic zones in metapelites and associated metatuffites. Illite crystallinity proved to be much more lithology-dependent than chlorite crystallinity, showing anomalously high IC values (anomalously low apparent grades) in certain metatuffites, as compared to metapelites. Massive metabasic rocks of lava or intrusive characters display anomalously high IC and ChC values.

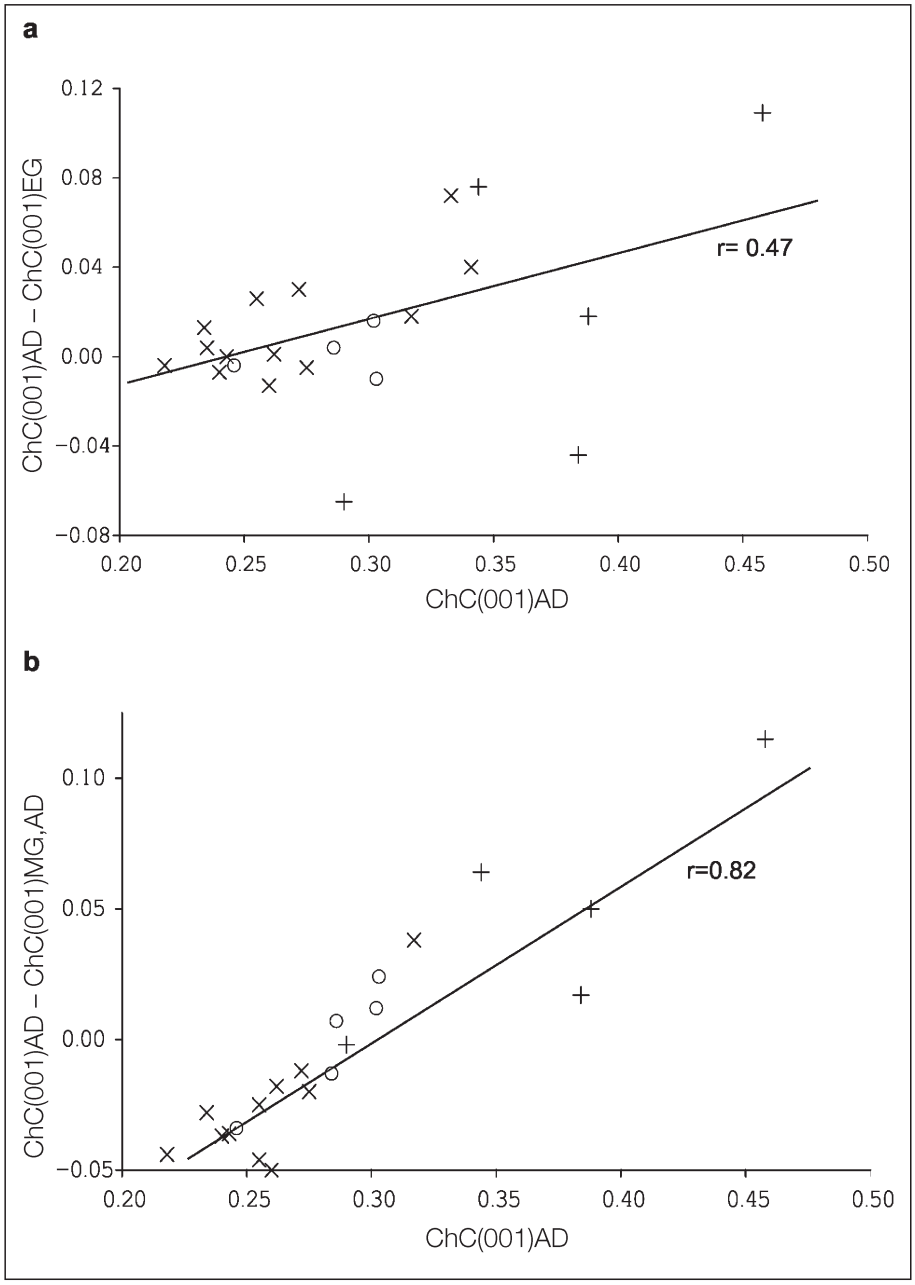

Text-Fig. 8.
Effects of glycolation (a) and Mg-saturation (b) on chlorite crystallinity, in function of metamorphic grade [ChC(001), AD].
Legend as in Text-Fig. 4.

2) Larger white K-mica and chlorite flakes and aggregates formed mostly in the cleavage (micro-shear) zones represent a more evolved stage in the reaction progress than the <2μm grain-size fraction, matrix-forming white K-mica and chlorite.
3) In addition to the well-known effect of decreasing amounts of smectitic mixed-layers in illite – white K-mica with increasing grade (temperature), celadonite content also strongly controls IC. With increasing celadonite content IC also increases. The celadonite content of illite – white K-mica is a function of bulk rock chemistry, correlating first of all with the $Al_2O_3/(Al_2O_3+FeO^*+MgO)$ ratio of bulk rocks.
4) Chlorite crystallinity reflects the integrated effects of swelling mixed-layers and dioctahedral (sudoitic) substitutions, while the Fe/Mg ratio of chlorites has no appreciable effect on ChC.

Out of the chlorite – bulk rock major element relations, the $Al_2O_3/(Al_2O_3+FeO^*+MgO)$ ratio seems to be strongly controlling both the ChC indices and the Al^{IV} and Al^{VI} contents of chlorite. Consequently, in addition to the evaluation of the effects of mixed-layers in chlorite, a strict bulk rock chemical control is needed when the chlorite-Al^{IV} content is applied for geothermometry.

As a consequence, bulk rock major element and mineral chemical relations should be taken into consideration when phyllosilicate crystallinity indices obtained from varying (mostly contrasting) lithologies are compared for deciphering diagenetic and incipient metamorphic conditions.

Acknowledgements

The authors are indebted to the "Stiftung Aktion Österreich-Ungarn", Budapest for financially supporting the joint field works and discussions by the grant No. 35öu8: "Comparative study of chlorite crystallinity and chemistry…") and the Austrian Academy of Sciences.

Thanks are due to Ms. V. VARGA for the bulk chemical analyses and for Mrs. O KOMORÓCZY, P.M. SÁNDOR, M. LÁTOS, Ms. K. TEMESVÁRI, N. KERESZTES and N. SZÁSZ (Laboratory for Geochemical Research, Hungarian Academy of Sciences) for their technical assistance and to P. HORVÁTH and E. KOBER for help in graphical work.

The laboratory work was sponsored by the Hungarian Scientific Research Fund (OTKA, Budapest), Project No. T-022773/1997-2000 to P.Á.

References

ALT, J.C. (1999): Very low-grade hydrothermal metamorphism of basic igneous rocks. – In: FREY, M. & ROBINSON, D. (eds.): Low-Grade Metamorphism, 169–226, Oxford (Blackwell Science).

ÁRKAI, P. (1991): Chlorite crystallinity: an empirical approach and correlation with illite crystallinity, coal rank and mineral facies as exemplified by Palaeozoic and Mesozoic rocks of northeast Hungary.– J. Metam. Geol. **9**, 723–734.

ÁRKAI, P., LELKES-FELVÁRI, Gy., LANTAI, Cs. & NAGY, G. (1995a): Biotite in a Paleozoic metagreywacke complex, Mecsek Mountains, Hungary: conditions of low-T metamorphism deduced from illite and chlorite crystallinity, coal rank, white mica geobarometric and microstructural data. – Acta Geol. Hung. **38**, 293–318.

ÁRKAI, P., MATA, M.P., GIORGETTI, G., PEACOR, D.R. & TÓTH, M. (2000): Comparison of diagenetic and low-grade metamorphic evolution of chlorite in associated metapelites and metabasites: an integrated TEM and XRD study. – J. Metam. Geol., **18**, 531–550.

ÁRKAI, P. & SADEK GHABRIAL, D. (1997): Chlorite crystallinity as an indicator of metamorphic grade of low-temperature meta-igneous rocks: a case study from the Bükk Mountains, northeast Hungary. – Clay Minerals, **32**, 205–222.

ÁRKAI, P., SASSI, F.P. & SASSI, R. (1995b): Simultaneous measurements of chlorite and illite crystallinity: a more reliable geothermometric tool for monitoring low- to very low-grade metamorphism in metapelites. A case study from Southern Alps (NE Italy). – Eur. J. Mineral., **7**, 1115–1128.

BETTISON, L.A. & SCHIFFMAN, P. (1988): Compositional and structural variations of phyllosilicates from the Point Sal ophiolite, California. – American Mineral., **73**, 62–76.

BUCHER, K. & FREY, M. (1994): Petrogenesis of metamorphic rocks. 6th edition. Complete revision of Winkler's textbook. – Berlin (Springer).

CATHELINEAU, M. (1988): Cation site occupancy in chlorites and illites as a function of temperature. – Clay Minerals, **23**, 471–485.

CATHELINEAU, M. & NIEVA, D. (1985): A chlorite solid solution geothermometer. The Los Azufres (Mexico) geothermal system. – Contr. Mineral. Petrol,. **91**, 235-244.

ESQUEVIN, J. (1969): Influence de la composition chimique des illites sur leur cristallinité. – Bull. Centre Res., Pau-SNPA 3, 147–153.

FLÜGEL, H. (1975): Die Geologie des Grazer Berglandes. Erläuterungen zur Geologischen Wanderkarte des Grazer Berglandes 1 : 100 000. – Mitt. Abt. Geol. Joanneum, Sh. **1**, 288, Graz.

FLÜGEL, H. & NEUBAUER, F. (1984): Steiermark – Geologie der österreichischen Bundesländer in kurzgefassten Einzeldarstellungen (Erläuterungen zur geologischen Karte der Steiermark 1 : 200.000). – Geol. B.-A., 127 S.

FREY, M. (1987): Very low-grade metamorphism of clastic sedimentary rocks. – In: FREY, M. (ed.): Low Temperature Metamorphism, 9–58, Glasgow (Blackie), .

FREY, M., DE CAPITANI, C. & LIOU, J.G. (1991): A new petrogenetic grid for low-grade metabasites. – J. Metam. Geol., **9**, 497–509.

FRITZ, H. (1986): Zur Geologie des nordwestlichen Grazer Paläozoikum (im Bereich Scharnerkogel – Parmaseggkogel). – Unveröff. Dissertation K.-F.-Univ. Graz, 209 S.

FRITZ, H. & NEUBAUER, F. (1988): Geodynamic aspects of the Silurian and Early Devonian sedimentation in the Paleozoic of Graz (Eastern Alps). – Schweiz. Mineral. Petrogr. Mitt., **68**, 359–367.

FRITZ, H. & NEUBAUER, F. (1990): „Grazer Paläozoikum". – Exk.-Führer, TSK III, 3. Symp. Tektonik, Strukturgeol. Kristallingeol., 24 S., Graz.

GOLLNER, H. (1985): Bericht 1984 über geologische Aufnahmen und biostratigraphische Untersuchungen im Paläozoikum auf Blatt 134 Passail. – Jb. Geol. B.-A., **128**, 292–293.

GSELLMANN, H. (1987): Zur Geologie am Nordostrand des Grazer Paläozoikums (im Bereich Hochschlag – Plankogel – Heilbrunn). – Unveröff. Dissertation K.-F.-Univ. Graz, 202 S.

HASENHÜTTL, C. (1994): Eine Wärmegeschichte des Grazer Berglands. Inkohlung, Illitkristallinität, Tonmineralogie und Conodont Colour Alteration Index im nördlichen Teil des Grazer Deckenkomplex (Grazer Paläozoikum, Österreich). – Unveröff. Dissertation K.-F.-Univ. Graz, 182 S.

HASENHÜTTL, C. & RUSSEGGER, B. (1992): Niedriggradige Metamorphose im Grazer Paläozoikum. – Jb. Geol. B.-A., **135**, 287–299.

HUBAUER, N. (1984): Bericht 1983 über geologische Aufnahmen im Hochlantschgebiet auf Blatt 134 Passail. – Jb. Geol. B.-A., **127**, 239–240.

HUBMANN, B. (1990): Die Fazies der Barrandeikalke (Grazer Paläozoikum). – Unveröff. Dissertation K.-F.-Univ. Graz, 243 S.

HUBMANN, B. (1999): Grazer Paläozoikum: Bibliographie 1819–1999. – Wien (Österr. Akad. Wiss)..

HUBMANN, B. & HASENHÜTTL, C. (1995): Zur Entwicklung der hohen Deckengruppe des Grazer Paläozoikums. Exkursionspunkte zu ausgewählten Profilen. – Exkursionsführer zur 2. Tagung Österr. Paläont. Ges., 43 S.

HUNZIKER, J.C., FREY, M., CLAUER, N., DALLMEYER, R.D., FRIEDRICHSEN, H., FLEHMIG, W., HOCHSTRASSER, K., ROGGWILER, P. & SCHWANDER, H. (1986): The evolution of illite to muscovite: mineralogical and isotopic data from the Glarus Alps, Switzerland. – Contrib. Mineral. Petrol., **92**, 157–180.

JIANG, W.-T., PEACOR, D.R. & BUSECK, P.R. (1994): Chlorite geothermometry? – Contamination and apparent octahedral vacancies. – Clays and Clay Min., **42**, 593–605.

JOWETT, E.C. (1991): Fitting iron and magnesium into the hydrothermal chlorite geothermometer. GAC/MAC/SEG Joint Annual Meeting, Toronto. – Program with Abstracts, **16**, A62.

KOLMER, H. (1978): Die Verteilung von Ti, Sr, Y und Zr in spilitischen Gesteinen der Steiermark. – Mitt. Naturwiss. Ver. Steiermark, **108**, 31–43.

KRANIDIOTIS, P. & MACLEAN, W.H. (1987): Systematics of chlorite alteration at the Phelps Dodge massive sulfide deposit, Matagami, Quebec. – Econom. Geol., **82**, 1898–1911.

LIOU, J.G., MARUYAMA, S. & CHO, M. (1987): Very low-grade metamorphism of volcanic and volcanoclastic rocks – mineral assemblages and mineral facies. – In: FREY, M. (ed.): Low Temperature Metamorphism, 59–113, Glasgow (Blackie).

LOESCHKE, J. (1989): Lower Paleozoic volcanism of the Eastern Alps and its geodynamic implications. – Geol. Rdsch., **78**, 599–616.

MERRIMAN, R.J. & PEACOR, D.R. (1999): Very low-grade metapelites: mineralogy, microfabrics and measuring reaction progress. – In: FREY, M. & ROBINSON, D. (eds.): Low-Grade Metamorphism. Oxford (Blackwell Science), 10–60.

NEUBAUER, F. (1981): Untersuchungen zur Geologie, Tektonik und Metamorphose des „Angerkristallins" und des E-Randes des Grazer Paläozoikums. – Jahresbericht 1980, Hochschulschwerpunkt S 15, **2**, 114–121.

NEUBAUER, F. (1982): Untersuchungen zur Tektonik, Metamorphose und Stellung des Grazer Paläozoikum-Ostrandes. – Jahresbericht 1981, Hochschulschwerpunkt S 15, **3**, 93–101.

REISINGER, J. (1988): I. Geologie des Hirschkogel-Landscha Berges nördlich von Weiz. II. Paläomagnetische Untersuchungen im Perm von St. Paul im Lavanttal und in der Kainacher Gosau. – Unveröff. Dissertation K.-F.-Univ. Graz, 176 S.

ROBINSON, D. & BEVINS, R.E. (1999): Patterns of regional low-grade metamorphism in metabasites. – In: FREY, M. & ROBINSON, D. (eds.): Low-Grade Metamorphism, Oxford (Blackwell Science), 143–168.

RUSSEGGER, B. (1992): Diagenese bis niedriggradige Metamorphose im südlichen Grazer Paläozoikum (Steiermark, Österreich). – Unveröff. Dissertation K.-F.-Univ. Graz, 180 S.

RUSSEGGER, B. (1996): Niedrigst- und niedriggradige Metamorphose im südlichen Grazer Paläozoikum (Ostalpen). – Jb. Geol. B.-A., **139**, 93–100.

SCHMIDT, S.T. & ROBINSON, D. (1997): Metamorphic grade and porosity and permeability controls on mafic phyllosilicate distributions in a regional zeolite to greenschist facies transition of the North Shore Volcanic Group, Minnesota. – Geol. Soc. Amer. Bull., **109**, 683–697.

THALHAMMER, O. (1983): Bericht 1982 über geologische Aufnahmen nördlich der Breitenau (Grazer Paläozoikum) auf Blatt 134 Passail. – Jb. Geol. B.-A., **126**, 316–317.

TSCHELAUT, W. (1984): Bericht 1981 über geologische Aufnahmen im NW-Teil des Grazer Paläozoikums auf Blatt 134 Passail. – Verh. Geol. B.-A., **1982**, A70–A71.

VIDAL, O. & PARRA, T. (2000): Exhumation paths of high pressure metapelites obtained from local equilibria for chlorite-phengite assemblages. – Geol. J., **35**, 139–161.

WEBER, L. (1990): Die Blei-Zinklagerstätten des Grazer Paläozoikum und ihr geologischen Rahmen. – Arch. Lagerst.forsch., **12**, 289 S.

WELISCH, L. (1911): Beitrag zur Kenntnis der Diabase der Steiermark. – Mitt. Naturwiss. Ver. Steiermark, **47**, 53–82.

WINKLER, H.G.F. (1979): Petrogenesis of metamorphic rocks. – 5th edition, New York (Springer).

YANG, C. & HESSE, R. (1991): Clay Minerals as indicators of diagenetic and anchimetamorphic grade in an overthrusted belt, external domain of southern Canadian Appalachians. – Clay Mineral., **26**, 211–231.

ZANG, W. & FYFE, W.S. (1995): Chloritisation of the hydrothermally altered bedrock at the Igarape Bahia gold deposit, Carajas, Brazil. – Mineral. Dep., **30**, 30–38.

Manuskript bei der Schriftleitung eingelangt am 5. März 2001